Terrain slugging in near horizontal oilwells

John Fozard

Jesus College

University of Oxford

A thesis submitted for the degree of

Master of Science

September 2001

Acknowledgements

I would like to thank my supervisor Andrew Fowler, and Paul Hammond and Gary Oddie from Schlumberger Cambridge Research for their helpful advice and encouragement. I also thank EPSRC and Schlumberger Cambridge Research for their financial support.

Abstract

In this thesis we consider the problem of terrain slugging in near horizontal producing wells. We formulate a simple model for stratified two-phase flow, and consider the linear stability of steady states. We then study the possibility of the formation of roll waves, and make a tentative attempt at a resolution of the problem.

Contents

List of Figures

Chapter 1

Introduction

1.1 The nature of the flow in wells

1.1.1 Oil-reservoirs

Hundreds of millions of years ago organic matter was deposited at the bottom of shallow tropical seas. Sediment from rivers was laid down on top of it, and under conditions of high pressure and increased temperature (50° to 70°) the organic matter was converted into hydrocarbons. The volatile (lower boiling point) hydrocarbons are gaseous in the form of natural gas, whereas the liquid fractions form oil. *Permeable* rocks such as sandstone have a porous structure that allow fluids to flow through them. Oil and gas accumulate in these rocks when they are prevented from rising by a layer of impermeable rock (such as rock salt) above them, and a reservoir of oil is formed. As the rock holding the oil is porous water also tends to be present in the reservoir.

1.1.2 Oil-wells

In order to extract the oil from a reservoir a well is drilled from the surface. Depending on the nature of the surrounding rock the well may be *open-hole* (simply a hole in the rock) or *completed* with a steel liner. Open-hole wells are usually only used to inject water into the reservoir. The oil and other substances in the reservoir enter the well at a number of producing regions. As a rule of thumb 95% of the production of the well enters along 5% of the length of the well. In the case of a lined well the products enter the well through *perforations* which are made using either shaped charges or specially constructed guns which are lowered down the well [1]. The inclination of the the well varies because of the properties of the rocks in the region and the distribution of the oil in the reservoir, and some wells consist of a near-horizontal section. However it

is not practical to drill the well dead straight, and such wells usually have a slowly undulating profile (the inclination of the well varying by at most 2° per 100m, which corresponds to a radius of curvature of about 2900m).

1.1.3 Water in oil wells

Over the operational lifetime of an oil well the proportion of water being produced by the well (the *water cut*) tends to increase. Water may encroach into the producing regions from a nearby aquifer, channel into the well from behind the casing, or travel along a fault in the rock formation. In some situations water is injected down into the reservoir in order to increase the production of oil. Commonly when the water cut increases the pressure drop (due to the pressure of the water in the permeable rocks above the reservoir) is insufficient to displace the oil (along with this undesired water) to the surface. When this is the case mechanical pumps have to be used, for instance an electronic submersible pump (ESP) placed down the hole, or a gas-lift system. It is clearly undesirable to expend energy lifting waste water along with the oil. Water may also sump in a dip and *kill* the well, preventing the production flow from passing this point and reducing output.

1.1.4 Production logging in wells

Due to the great expense involved in drilling and operating a well and the value of the product, oil extraction companies use a number of techniques to improve the output and extend the profitable operational lifetime of the well. New perforations can be introduced or old ones sealed off over specific sections and side wells may be opened or shut off.

However in order to know which techniques will be effective it is necessary to determine where water and oil are being produced, and the properties of the flow in the well. This is accomplished using a production logging (PL) tool, which consists of a large string of sensors which travels slowly along the well and gives a time averaged view of the flow, as shown in figure 1.1. The sensors measure the *holdup* (proportion of the cross-section occupied) of the phases, and the flow rates of the phases present. Sometimes it is not possible to measure the flow rates of all the phases directly, and the unknown data have to be deduced from the other measurements, which requires an accurate model of the flow as in [44].

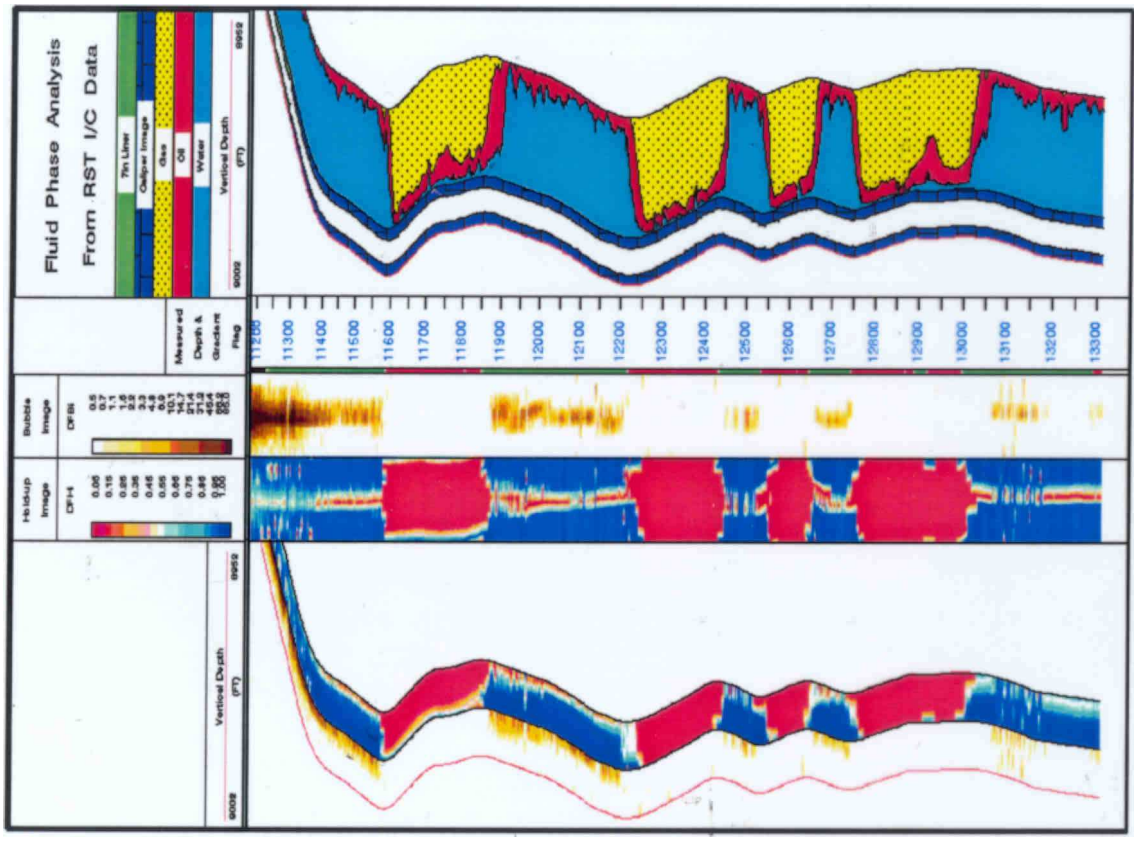

Figure 1.1: Production logging data from a near horizontal well. The top plot shows both the undulating profile of the well and the hold-ups of each of the phases present (all three of oil, water and gas in the case of this well) measured by a reservoir saturation tool, which bombards the flow with neutrons and measures the gamma rays emitted by the fluids. The next two plots down show the number of bubbles present and more hold up data respectively, this time measured by conductance probe placed at four equally spaced points around the perimeter of the liner. At the bottom this data has been superimposed on the well profile. From this we can see that the majority of the cross section is occupied by gas in the downwards sections and water in the uphill sections. See [5] for more details

1.2 The problem

BP operate an number of oil wells in the Wytch Farms oil-field. In a pair of near-horizontal wells there it was found that over time the proportion of water cut increased and the total flow rate decreased [8]. This precipitated a major change in the behaviour of the flow. The flow-rate at the output varied periodically (with period of about 20 minutes, as can be seen in figure 1.3). This is known as severe terrain slugging, and the variation in the mass flowput causes increased wear and possibly damage to the pumps in the well. Such pumps are extremely expensive, and difficult to access. The periodic behaviour also causes difficulty in interpreting production logging results.

The slugging is though to be generated by the undulations in the pipeline. The topography of the well M5 is shown in figure 1.2, where we can see that the well consists of an undulating near-horizontal section of about 900 m in length, and then a steeper section rising at about 10° up to the pump. Simulations using a numerical model (OLGA) for this well showed slugs of water being generated, which had a period of about 1 minute. However the numerical calculation did not show the long-period oscillations in the total volume flowput, nor give much information as to the physical process generating these slugs. This behaviour was considered to be unusual, as in oil-water flows slugging is generally not observed in straight pipes under experimental conditions, and stratified flow (with some amount of mixing) is possible in a straight pipe at these flow rates and inclinations.

1.3 Two-phase flow

1.3.1 Flow phenomena

Two-phase flow exhibits phenomena not present in single phase flow, as when more than one fluid is present the interface may adopt one of a number of different geometrical configurations, and so different *regimes* occur. The typical regimes for horizontal gas-liquid flow are outlined in Whalley [49]. Note that this is a very simplistic classification, and other authors such as Spedding and Spence [39] have distinguished over 12 distinct flow patterns. Usually the regime is determined by visual observation, and so the classification is quite subjective. However changes in the regime can have dramatic results, for example the pressure drop in slugging air-water flow is about twice that of a similar stratified flow. In oil-water flow the types of regimes observed

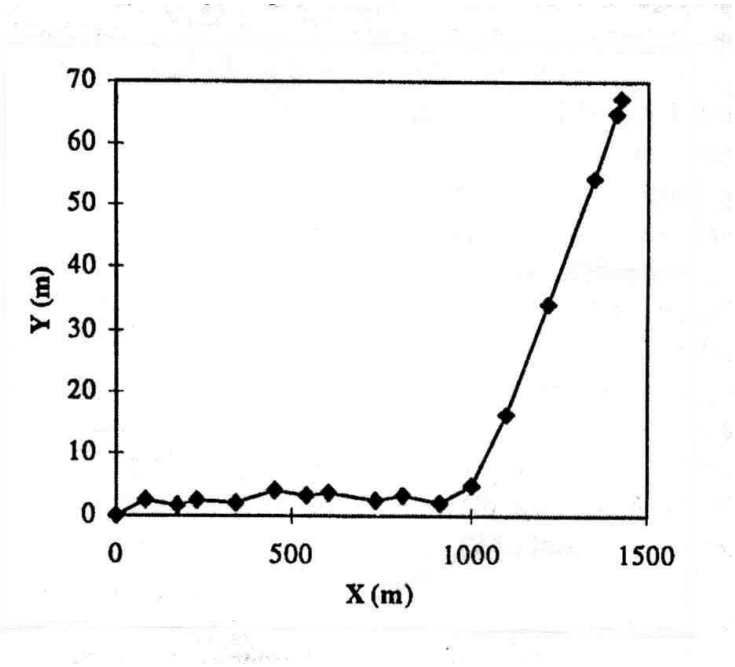

Figure 1.2: A plot of vertical height (measured upwards from the bottom of the well) against distance along the well. This was the data used for the simulations in [8], and it shows the slowly varying inclination (although in [8] the profile was taken to be as coarse as possible, as it was felt that this was the cause of the slugs).

are very different as the much smaller density difference allows the phases to mix and form dispersions more readily, as noted in [45].

1.3.2 Experimental studies of oil-water flow

Oil-water flows have been of commercial importance for some time. It was found that the introduction of a small amount of water in a long distance transport pipeline reduces the total frictional pressure drop along the pipeline, and so decreasing the amount of energy required to pump the oil, as patented by Isaacs and Speed in 1904. The oil in such pipelines typically has a much greater viscosity than the water, and the water forms an annular region around a cylindrical core of water, reducing the stresses at the walls. Such flows have been studied by Charles *et al.* [13] and Hasson *et al.* [23].

There are a large number of parameters affecting oil-water flows, such as pipe diameter, flow rates, viscosity and density of the two fluids, surface tension, and the angleof inclination of the flow, and due to the cost of the equipment experimental studies tend to be very limited in the range over which these parameters are varied. Typically in a given study the pipe diameter and material are fixed, along with the

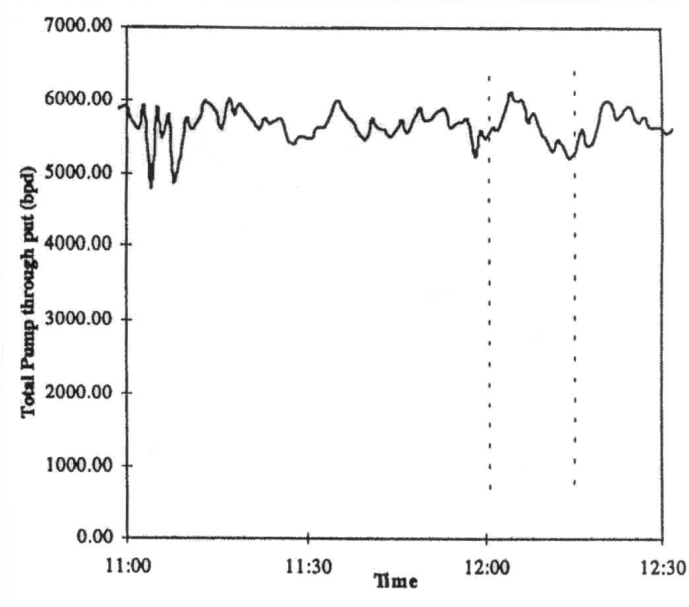

Figure 1.3: The total flow rate at the output of well M5 over time, showing oscillations of period about 20 minutes. From [8].

type of oil used. There is a considerable *entrance length* of the pipe (of the order of 200 pipe diameters) over which the flow is strongly effected by the conditions at the inlet, and so in order to view a fully developed regime a very long pipe is required. For this reason most studies use a horizontal pipe, as varying the inclination of a long pipe causes considerable practical difficulties.

Russell *et al.* [36] conducted the first experiments into oil-water flows, and managed to classify flows as mixed, bubbly and stratified flows. Subsequently, Charles *et al.* [13] studied flows where both oil and water were of equal density in a pipe of 0.025m internal diameter (i.d.) and Hasson *et al.* [23] studied the break up of a core annular flow in a pipe of 0.0126m i.d. Slug flow was noted in these two studies, but in the form of large bubbles in the centre of the pipe. These appear to have more in common with plug flow than the turbulent travelling waves found in air-water flow, and may well only be observed due to the artificial inlet conditions or lack of density difference between the phases.

In the majority of other experiments conducted the flow regimes observed were similar to those of Trallero's [45] who used a pipe of 0.050 m id, and an oil of viscosity 20 mPa s for horizontal flow. Kurban *et al.* [26] and Angeli and Hewitt [2] performed experiments with a oil of 1.6 mPa s viscosity and 801 kg/m^3 density and in a pipe of i.d. 0.024m. Fairuzov *et al.* [20], conducted experiments in a much larger diameter

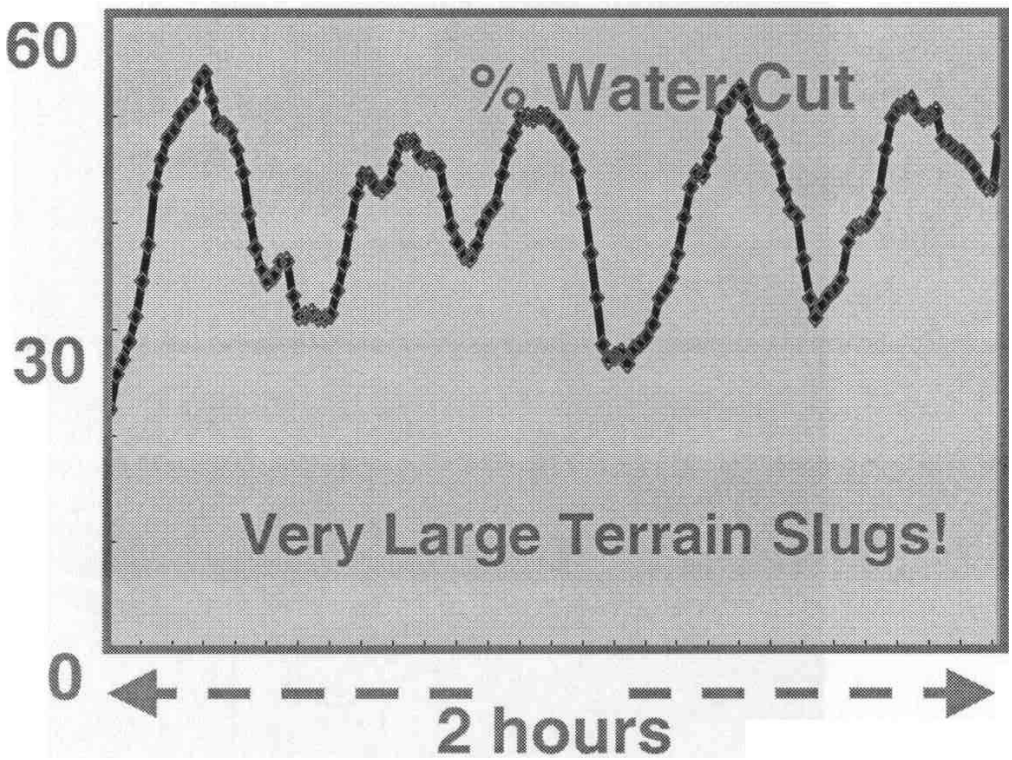

Figure 1.4: Water cut against time from a similar well undergoing terrain slugging.

pipe (0.3635 m) and with a low viscosity oil. In this study the flow was typically dispersed, although stratified flow was noted at moderate flow rates (less than about 1.5ms^{-1}). However for low water fractions (less than 3 percent) the water was dispersed in the oil, forming a layer at the bottom of the pipe. Nadler and Mewes [33] performed experiments in a small diameter (0.059m) pipe, concentrating on pressure drops for dispersed flows. Other experiments have been conducted by Schlumberger Cambridge Research, and a basic outline of the results can be seen in the article "Fluid Flow Fundamentals" [12].

1.4 Regimes in near-horizontal oil-water flow

A simple classification for near-horizontal oil-water flows was presented in Trallero's thesis [45], and outlined further by Fairuzov *et al.* [20] and Nadler and Mewes [33]. This only includes the regimes observed in a straight flow-loop at small angles to the horizontal, and for oils of moderate viscosity ($<$ 30 cP). Core-annular flow as discussed previously tends to only occur when there is a much greater difference in viscosity between the phases. In highly deviated and vertical flows we expect different regimes to occur, in particular a form of rolling wave motion. However surprisingly

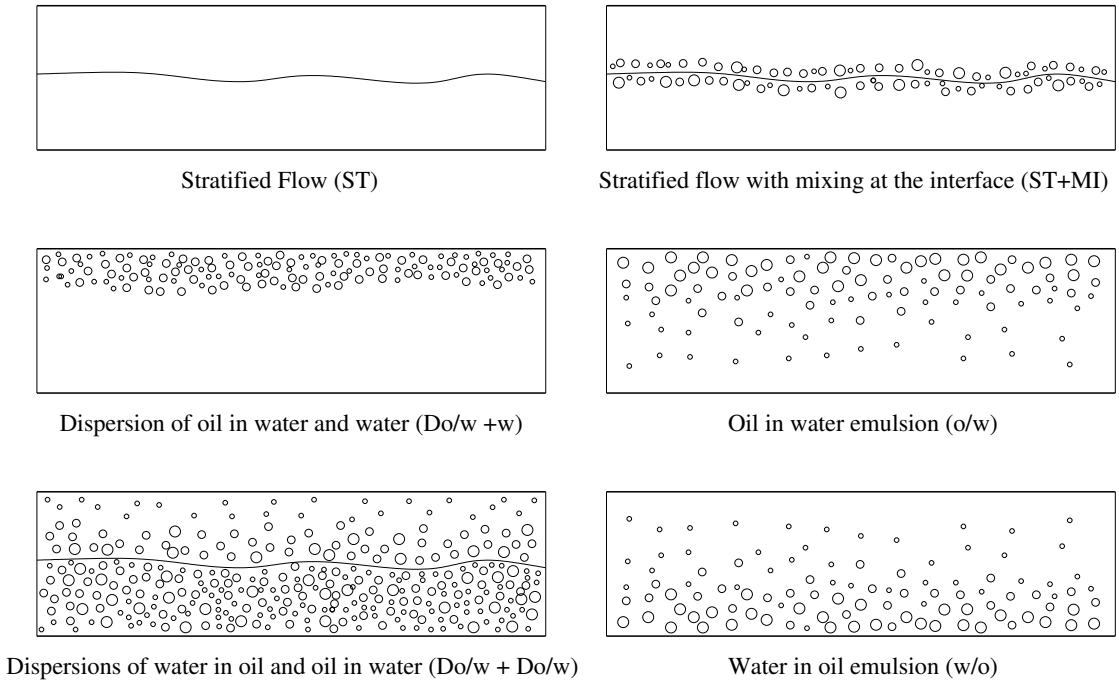

Figure 1.5: Regimes in oil-water two phase flow. After Trallero *et al.* [46].

slug flow was not observed at moderate angles of inclination [45]. Sketches of the different regimes may be seen in figure 1.5.

1.4.1 Segregated flow

At low flow rates the effect of gravity is dominant, and *stratified flow (ST)* occurs. The lighter phase is in the upper half of the pipe cross section, with a smooth interface. At higher flow rates waves develop on the interface. A small mixing region near the interface develops, where bubbles of water are found in the oil phase, and vice-versa, but apart from this the phases are segregated. This is known as *stratified flow with mixing at the interface (ST+MI).*

1.4.2 Dispersed Flow

At higher flow rates (and also when the water fraction is very large or small) the turbulent mixing is sufficiently intense to disperse one or both phases. Trallero [45] distinguishes dispersions and emulsions, the difference between the two being that a dispersion will settle out within the time scale being considered, whereas emulsions are effectively stable. He also classes the regime as an emulsion when one of the phases is totally dispersed within the other. At very high flow rates there is either an *oil in*

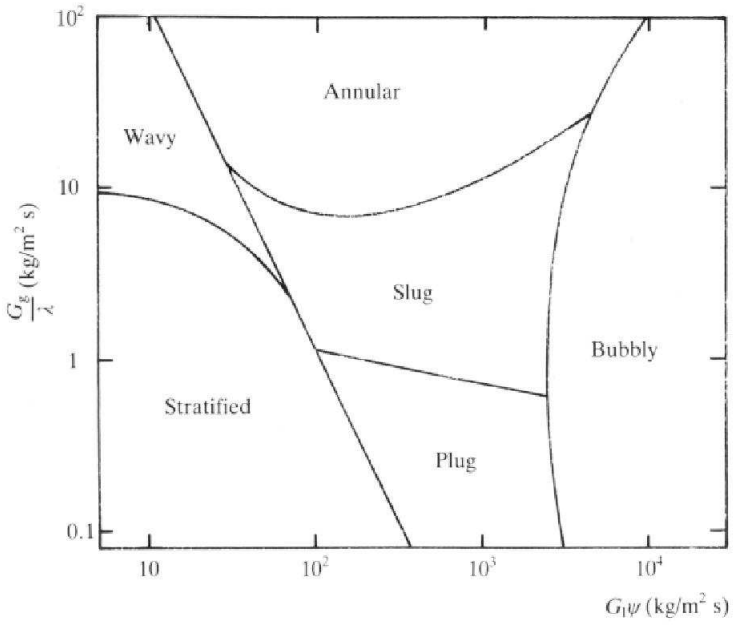

Figure 1.6: The Baker map for horizontal gas-liquid flow in a tube. Here $\lambda = (\frac{\rho_g}{\rho_a}\frac{\rho_l}{\rho_w})^{\frac{1}{2}}$ and $\psi = \frac{\sigma_w}{\sigma}\left(\frac{\nu_l}{\nu_w}\left[\frac{\rho_w}{\rho_l}\right]\right)^{\frac{1}{3}}$, where the subscripts w,a,l,g denote the properties of water, air, and the liquid and gas under consideration respectively. After [49].

water emulsion (o/w) or a *water in oil emulsion (w/o)*, dependent on the proportion of water. As the amount of water flowing varies a *phase inversion* may occur between these two regimes. When there is a significant difference in the viscosities of the fluids this may result in a decrease in the pressure drop along the pipe.

For intermediate flow rates there is a balance between these two processes, and a *dispersion oil in water over water (Do/w + w)* or a *dispersion of water in oil over a dispersion of oil in water (Dw/o + D o/w)* may occur.

1.5 Regime Diagrams

A number of attempts have been made to attempt to predict the regime type in two-phase flow, typically in the form of a regime diagram or map. The most famous of these is the Baker map [4], which was subsequently modified by Scott [38] (see figure 1.6).

This assumes that the flow type depends only on the two mass fluxes G_l and G_g, the surface tension σ, and the viscosities of the two fluids. However the flow regime is determined from a pair of dimensional quantities and so is limited in its range of applicability. Such regime diagrams are usually produced from experimental

results in a *flow-loop*, which consists of a straight, usually partially transparent pipe through which fluids can be pumped in a controlled manner. The flow rates and the *hold-up* (fraction of cross section occupied) of each of the phases present can be measured accurately, and the overall regime can be easily observed. The flow loop at Schlumberger Cambridge Research may be inclined at any angle in-between -1° downwards and vertically upwards. The regime diagram for the Baker map was derived from the experimental results of a number of authors, for liquid and low density gas, and mainly from experiments in small (0.0254 m) diameter pipes. As noted in [39] pipe diameter has a significant effect on the regime transition boundaries. Taitel and Dukler [43] produced a more complicated type of "map", with criteria which depend on the values of a number of dimensionless groups. They applied an empirical modification of the Kelvin-Helmholtz criterion for the instability of two-layer inviscid parallel flow between two rigid plates as a criterion for stability of stratified flow.

A comprehensive review of the different maps produced for gas-liquid flow has been conducted by Spedding and Spence [39]. The observed regime depends greatly on the inclination of the pipe. For near vertical flows other regimes such as churn flow can occur, and even for near-horizontal flows the a small inclination of the pipe has very significant effect. In gas-liquid systems flows inclined slightly upwards usually exhibit slugging, whereas slightly downwards flows are usually stratified [52].

1.6 Terrain slugging

Undulating or hilly pipelines cause terrain slugging. This has been studied by a number of authors [42], [37] for gas-liquid flows, but in the majority of these studies the pipeline has a near vertical $(80^\circ - 90^\circ)$ uphill section before the outlet. The paper [16] has an interesting experimental account of the mechanisms operating in such gas-liquid slugging, both for undulating pipelines and pipeline-riser systems. Water fills the upwards sections of the pipeline, and when the pressure of the gas compressed behind it is sufficiently high the water is flushed out in a series of slugs. At lower gas flow rates the water also builds up in the section of pipe leading down to the riser. However the build up of pressure via compression of the gaseous phase plays an important role in this mechanism, and for our oil-water flow we expect such effects to be negligible. Another significant difference is that the pipeline in such models and experiments consists of a number of straight sections joined together by sharp bends, as opposed to the slowly undulating well in our problem.

Chapter 2

A simple model for stratified two phase flow

2.1 Modelling two phase flow

In this chapter we will formulate a simple one-dimensional two-phase flow model, which will be very similar to those used by Barnea *et al.* [7], and a model supplied by Schlumberger Cambridge Research.

Our model will apply to a flow consisting of two distinct incompressible fluids, namely oil and water, where oil is the less dense phase. Where necessary we will use the subscript w to denote water and o to denote oil. The same model is often used when one of the phases is compressible (for instance air-water flow), as long as the velocities being observed are much smaller than the sound-speed.

Assume that the pipe is smooth, and circular in cross-section. We choose a set of orthogonal coordinates, with the x-axis along the pipe, the y-axis horizontal in the plane of the cross-section of the pipe, and the z-axis pointing upwards. In order to produce a one-dimensional problem we then assume that, after we have averaged over a suitable time scale, the two phases have a simple distribution in each cross section with a flat interface. This is shown in figure 2.2, where the wetted perimeters S_o and S_w, the interface width S_I and the interface height h_I are defined. This assumption of a flat interface is discussed in [35] for laminar flow of the two phases, and is deemed to be a good approximation for large Bond number $B = \frac{\Delta\rho g a^2}{\sigma}$, where $\Delta\rho$ is the difference in the densities of the phases, g the gravitational constant, a the pipe radius and σ the surface tension in between the two phases.

Define A to be the fraction of the cross-section of the pipe occupied by the water phase, and A_c to be the total cross-section of the pipe. We will assume that any effects due to the curvature of the pipe are negligible, for as noted earlier the radius

of curvature of the pipe is huge. A vertical cross-section down the middle of the pipe is shown in figure 2.1, and we take α to be the angle of inclination from horizontal, with α positive for downwards pipe inclination.

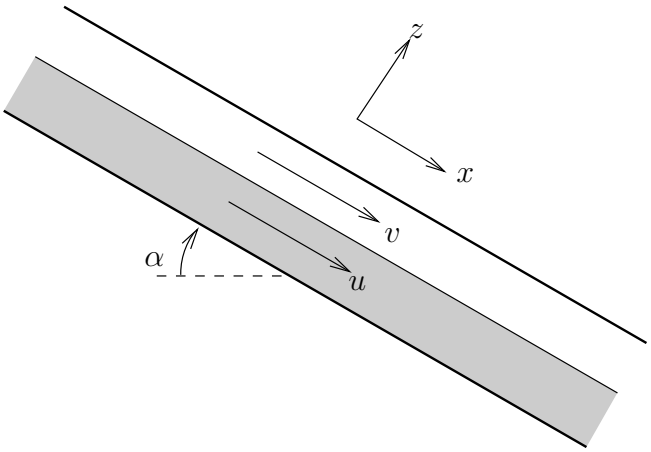

Figure 2.1: A vertical cross-section through the pipe

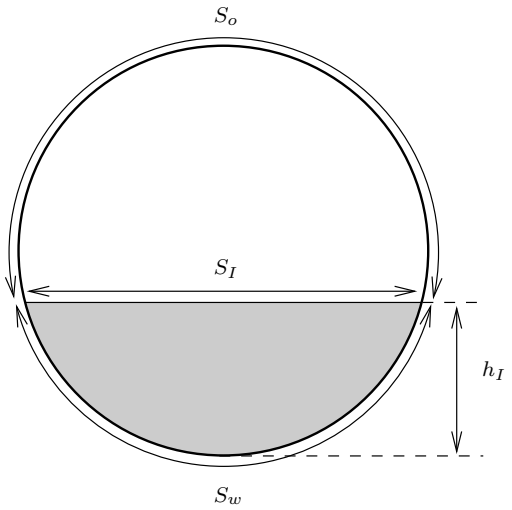

Figure 2.2: Assumed time-averaged distribution of the two phases in a cross section of pipe

Let $u(x,t)$ be the average (over the cross-section) of the component of direction of increasing x of the water velocity, and $v(x,t)$ the average velocity of the oil. Similarly define p_w and p_o to be the mean pressures in each phase, and p_I to be the mean pressure at the interface. Oil and water pass into the pipe through perforations made in the lining, and to model this we let q_w and q_o be the (volume) rate of inflow per unit length of the pipe of water and oil respectively.

Now consider the region of the pipe in between $x = a_1(t)$, and $x = a_2(t)$. If $\dot{a_1} = u(a_1, t)$ and $\dot{a_2} = u(a_2, t)$ then by the definition of the average velocities there is no net mass flux through $x = a_1(t)$ and $x = a_2(t)$, and so conservation of mass in this region gives

$$A_t + (Au)_x = \frac{q_w}{A_c}. \tag{2.1}$$

Similarly for the oil phase we have

$$(1 - A)_t + ((1 - A)v)_x = \frac{q_o}{A_c}. \tag{2.2}$$

We now consider conservation of momentum in the direction along the pipe for the same region of fluid. If the flow is not uniform across the cross-section of the pipe there is a non-zero momentum flux through a boundary given with speed u, as the average of u^2 is greater than the square of the average of u. We introduce a constant profile coefficient $D > 1$ to account for this, where $D = \frac{\int \hat{u}^2 dydz}{AA_c u^2}$.

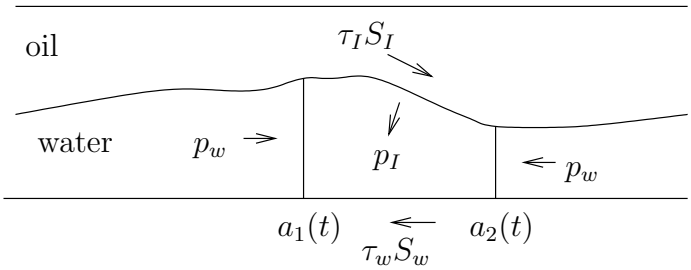

Figure 2.3: Diagram for momentum considerations

The forces acting on this region of water are the pressure of the water at the two ends, the interfacial pressure on the boundary with the oil, and lateral stress terms at the interface and on the boundary with the wall. Thus considering conservation of momentum now gives

$$\frac{d}{dt}\left(\int_{a_1}^{a_2} \rho_w u A A_c \, dx\right) = \int \tau_w S_w \, dx + \int \rho g \sin\alpha A A_c \, dx \tag{2.3}$$

$$-[\rho A A_c (D-1) u^2]_{a_1}^{a_2} - [p_w A A_c]_{a_1}^{a_2} - \int p_I S_I \mathbf{n}.\mathbf{i} \, ds + \int \tau_I S_I \mathbf{t}.\mathbf{i} \, ds, \tag{2.4}$$

where s is arc length along the interface. On the interface $\mathbf{n}$ is the unit normal pointing from the water into the oil, and $\mathbf{t}$ is the unit tangent vector (in the direction

of increasing x). Now $ds = \sqrt{1+(\frac{\partial h_I}{\partial x})^2}$, $\mathbf{n}.\mathbf{i} = -\frac{\frac{\partial h_I}{\partial x}}{\sqrt{1+(\frac{\partial h_I}{\partial x})^2}}$, $\mathbf{t}.\mathbf{i} = \frac{1}{\sqrt{1+(\frac{\partial h_I}{\partial x})^2}}$, and so we have

$$\begin{aligned}\int_{a_1}^{a_2} \frac{\partial}{\partial t}(\rho_w u A A_c) + \frac{\partial}{\partial x}(D\rho_w u^2 A A_c)\ dx &= \int_{a_1}^{a_2} (\tau_w S_w + \tau_I S_I \\ &\quad -\frac{\partial}{\partial x}(p_w A A_c) + p_I S_I \frac{\partial h_I}{\partial x})\ dx.\end{aligned} \tag{2.5}$$

Using $S_I = A_c \frac{dA}{dh_I}$, and $-\frac{\partial (A p_w)}{\partial x} + \frac{\partial A}{\partial x} p_I = -\frac{\partial A}{\partial x}(p_w - p_I) - A\frac{\partial p_w}{\partial x}$, we obtain

$$\begin{aligned}\rho_w((Au)_t + (D_w A u^2 + A h_w g\cos\alpha)_x) &= -A\frac{\partial p_I}{\partial x} + \rho_w g A \sin\alpha \\ &\quad + \frac{\tau_I S_I}{A_c} - \frac{\tau_w S_w}{A_c}.\end{aligned} \tag{2.6}$$

Similarly for the oil phase momentum we obtain the equation

$$\begin{aligned}\rho_o(((1-A)v)_t + D_o(1-A)v^2 + ((1-A)h_o g\cos\alpha)_x) &= -(1-A)\frac{\partial p_I}{\partial x} \\ &\quad + \rho_o g(1-A)\sin\alpha - \frac{\tau_I S_I}{A_c} - \frac{\tau_o S_o}{A_c}.\end{aligned} \tag{2.7}$$

2.1.1 Pressure considerations

If we assume that the vertical components of the acceleration of the two fluids are small (compared with g) then the z component of the Reynolds turbulence equations [40] give us that the pressure is hydrostatic in each phase, i.e. that

$$\frac{\partial p_k}{\partial z} = -\rho_k g\cos\alpha, \tag{2.8}$$

(where $k = o, w$ denotes the phase under consideration) and this assumption will be valid provided the slope of the interface is small. From this assumption we have that

$$\int_k (p_k - p_I)\ dy\ dz = \rho_k g \int_k (h_I - z)\cos\alpha\ dy\ dz, \tag{2.9}$$

(where here $\int_k dy\ dz$ denotes the integral over the part of the pipe cross section occupied by the phase k) and if we define h_w and h_o as

$$A_c A h_w = \int_w (h_I - z)\ dy\ dz, \qquad A_c(1-A)h_o = \int_o (h_I - z)\ dy\ dz, \tag{2.10}$$

then h_w and $-h_o$ are the distances of the centres of pressure of each phase from the interface, and for $k = o, w$

$$\int_k (p_k - p_I)\ dy\ dz = \rho_k g A_k h_k. \tag{2.11}$$

Some useful identities in manipulating these expressions are

$$\frac{d}{dA}(Ah_w) = A\frac{dh_I}{dA}, \qquad \frac{d}{dA}((1-A)h_o) = (1-A)\frac{dh_I}{dA}. \tag{2.12}$$

Typically the fluid in the reservoir is moving slowly, and so is at hydrostatic pressure. As the difference between the densities of the two phases is not large, we rescale

$$p_I \;=\; p_h + p, \tag{2.13}$$

where p_h is hydrostatic pressure at the midpoint of the well and so $\frac{dp_h}{dx} = \rho_w g \sin\alpha$.

2.1.2 Stresses on the phases

The shear stresses due to viscous effects on the walls of the pipe and at the interface between the two fluids are usually modelled in the form

$$\tau_w = \frac{1}{2}\rho_w f_w u\,|u|, \qquad \tau_o = \frac{1}{2}\rho_o f_o v\,|v|, \qquad \tau_I = \frac{1}{2}\rho_o f_I (v-u)\,|v-u|, \tag{2.14}$$

which are derived from empirical observations and application of Prandtl's mixing length formula. In engineering literature the Fanning friction factors f_w and f_o are functions of the Reynolds number of the flow, and are usually chosen to be the same as the friction factor for the corresponding single phase flow. From experimental studies this is a complicated function of the Reynolds number and the pipe roughness (see [28]). However for turbulent flow in a smooth pipe the simpler modified Blasius correlation is usually used for stratified two phase flow,

$$f \;=\; CRe^{-m} \tag{2.15}$$

where

$$Re_w = \frac{4uAA_c}{\nu_w S_w} \qquad Re_o = \frac{4v(1-A)A_c}{\nu_o(S_o+S_I)} \tag{2.16}$$

and [43] and [7] use $C = 0.046$, $m = 0.2$. Although these are merely estimates for the Reynolds numbers of the phases, they come from an analogy with open channel flow for the water phase, and closed channel flow for the liquid phase. This relation for the frictional terms was used by Kurban *et al.* [26], but other authors [11] and [10] use adjustable definitions for the hydraulic diameters, treating the faster phase as closed channel flow and the slower phase as open channel flow. In addition they assume that the interfacial frictional term uses the same friction factor and density term as the faster phase. More complicated correlations are sometimes used for the interfacial stress, as it is affected by the presence of waves and mixing at the interface.

For instance for gas-liquid flows at high gas flow rates Taitel and Dukler [43] used $f_I = 0.016$ or $f_I = f_g$ if $f_g > 0.016$. Alternatively f_I is sometimes considered to be as large as $10 f_g$ due to the influence of waves on the interface (see [14]). More accurate expressions for oil-water flow have been determined experimentally by [44], who used a correlation based on the internal Reynolds number and internal Froude number of the two phases. Such a model is only really necessary in determining the position of the equilibria accurately in stratified steady two phase flow, and the values of the coefficients used are commercially sensitive. For simplicity we will choose $f_I = f_o$ at all times. We will also assume that $f_o = k_o$ and $f_w = k_w$ where k_w and k_o are constant, but use the modified Blasius correlation to determine a rough estimate of their sizes. We will choose k_w and k_o to be the values that the friction factors would take if each phase was flowing alone and occupying the whole cross section of the pipe, namely

$$k_w = C\left(\frac{Q_w d}{\nu_w}\right)^{-0.2}, \qquad k_o = C\left(\frac{Q_o d}{\nu_o}\right)^{-0.2}. \tag{2.17}$$

An issue may arise regarding the transition to/from turbulent flow in each phase. The flow is typically deemed to be turbulent for Reynolds numbers greater than 3000. For the pipe diameter considered in this thesis ($d = 0.14$m), this corresponds to a water velocity of more than 0.01ms^{-1} or 80bpd and an oil velocity of more than 0.02ms^{-1} or 160bpd, when each phase is flowing individually. From the definition of the Reynolds numbers we see that, for a given volume flux (or superficial velocity) of a phase the Reynolds number is always greater in a stratified two phase flow than when the fluid is flowing alone in the pipe, and so provided the preceding relations hold both phases are likely to be turbulent. For a turbulent flow we assume that $D \simeq 1$ and so ignore the effects of profile coefficients.

2.2 Non dimensionalisation

In order to non dimensionalise the problem scale

$$x = [x]x^*, \quad t = [t]t^*, \quad u = [u]u^*, \quad v = [v]v^*, \quad p = p_0 + [p]p^*. \tag{2.18}$$

following [15]. We attempt to balance the water momentum term against the wall stress on the water phase, and this gives us a length scale of $d/2f_w$. Choosing a typical velocity U for the velocity scale and a convective time scale we have

$$p = \rho_w[u]^2, \quad [x] = \frac{d}{2k_w}, \quad [t] = \frac{[x]}{[u]}, \quad [u] = U. \tag{2.19}$$

The pressure is scaled to balance the acceleration term in the water momentum equation. Then we have the following dimensionless parameters

$$r = \frac{\rho_o}{\rho_w}, \quad \delta = \frac{k_w}{k_o} = \left(\frac{\nu_w}{\nu_o}\right)^{0.2}, \quad \beta = \frac{gd}{U^2}, \quad \gamma = \frac{gd}{2k_w U^2}, \tag{2.20}$$

and (on dropping the asterisks) the dimensionless equations are of the form

$$\begin{aligned}
-A_t + ((1-A)v)_x &= q_o, && (2.21)\\
A_t + (Au)_x &= q_w, && (2.22)\\
v_t + vv_x + \frac{\beta}{1-A}((1-A)h_o g\cos\alpha)_x &= -\frac{1}{r}\frac{\partial p}{\partial x} + \gamma(1-\frac{1}{r})\sin\alpha && (2.23)\\
&\quad -\frac{(v-u)\,|v-u|\,S_I}{\pi\delta(1-A)} - \frac{v\,|v|\,S_o}{\delta(1-A)}\\
&\quad -\frac{q_o v}{1-A},\\
u_t + uu_x + \frac{\beta}{A}(Ah_w g\cos\alpha)_x &= -\frac{\partial p}{\partial x} && (2.24)\\
&\quad +\frac{r(v-u)\,|v-u|\,S_I}{\pi\delta A} - \frac{u\,|u|\,S_w}{A}\\
&\quad -\frac{q_w u}{A}.
\end{aligned}$$

Note that we also scale

$$S_o = \pi d S_o^*, \qquad S_w = \pi d S_w^*, \qquad S_I = d S_I^*, \tag{2.25}$$

(so S_o, S_w and S_I vary between 0 and 1) and

$$Q_o = A_c U Q_o^*, \qquad Q_w = A_c U Q_o, \qquad Q = A_c U Q_o, \tag{2.26}$$

$$q_o = \frac{A_c U}{[x]} q_o^*, \qquad q_w = \frac{A_c U}{[x]} q_w^*, \tag{2.27}$$

so Q_o and Q_w are the dimensionless *superficial velocities* (volume flux per unit cross sectional area) of each phase. Here δ and r are properties of the fluid pair only, whereas γ and β depend on the pipe diameter, the flow rate and the friction factor for the water phase.

2.2.1 Typical flow parameters

For oil-water flow through the well M5 at Wytch farms the properties of the water and gas phases are

$$\rho_w = 1100 \text{ kg m s}^{-1} \tag{2.28}$$

$$\mu_w = 0.5 \times 10^{-3}\text{Pa s} \tag{2.29}$$
$$\nu_w = 4.55 \times 10^{-7}\text{m}^2\ \text{s}^{-1} \tag{2.30}$$
$$\rho_o = 750\ \text{kg m s}^{-1} \tag{2.31}$$
$$\mu_o = 1.02 \times 10^{-3}\text{Pa s} \tag{2.32}$$
$$\nu_o = 1.36 \times 10^{-6}\text{m}^2\ \text{s}^{-1} \tag{2.33}$$

The flow was taking place in a well with

$$d = 0.14\ \text{m} \tag{2.34}$$

and the oil flow-rate through the well was 3472bpd with a 46% water cut (where bpd denotes barrel per day, and 1 barrel = 0.1591m^3, so 1bpd = $1.8414 \times 10^{-6}\text{m}^3\text{s}^{-1}$). The cross sectional area of the pipe is $A_c = 0.0154\text{m}^2$ and therefore

$$Q_o = 0.42\ \text{ms}^{-1} \tag{2.35}$$
$$Q_w = 0.35\ \text{ms}^{-1} \tag{2.36}$$
$$k_o = 0.0048 \tag{2.37}$$
$$k_w = 0.0039 \tag{2.38}$$

and so we have scales

$$[x] = 18\ \text{m}, \quad U = 0.77\ \text{m s}^{-1}, \quad [t] = 23\ \text{s}. \tag{2.39}$$

These then give us the dimensionless parameters

$$r = 0.68, \quad \beta = 2.3, \quad \gamma = 290, \quad \delta = 1.2, \tag{2.40}$$
$$Q = 1, \qquad Q_o = 0.54, \qquad Q_w = 0.45. \tag{2.41}$$

2.3 Simplification of equations

We can immediately integrate the sum of (2.21) and (2.22) to give

$$Au + (1 - A)v = Q(t) + \int_0^x q\ dx = Q^*(x, t) \tag{2.42}$$

where Q^* is the total (non-dimensional) volume flux per unit cross sectional area (or mean velocity) through the pipe. This relationship can be used to eliminate v in (2.24) and (2.25) to give

$$A_t + (Au)_x = 0, \tag{2.43}$$
$$g_1 u_t + g_2 u_x + g_3 A_x = f, \tag{2.44}$$
$$\tag{2.45}$$

where

$$g_1 = 1 + \frac{rA}{1-A}, \tag{2.46}$$

$$g_2 = u + \frac{rA}{(1-A)^2}((1-A)u + 2(Q^* - u)), \tag{2.47}$$

$$g_3 = -r\frac{(Q^*-u)^2}{(1-A)^3} + \beta(1-r)\cos\alpha(x)\frac{dh_I}{dA}, \tag{2.48}$$

$$\begin{aligned} f &= (1-r)\gamma\sin\alpha(x) + \tau_I(\frac{1}{A} + \frac{1}{1-A})S_I + \frac{\tau_o S_o}{\delta(1-A)} - \frac{\tau_w S_w}{A} \\ &\quad + \frac{r}{(1-A)^2}(Q_t^*(1-A) + q_w(Q^*-u) + q(Q^*-Au)) - \frac{q_w u}{A} + \frac{rq_o}{(1-A)^2}(Q^*-Au). \end{aligned} \tag{2.49}$$

(here we have neglected terms containing $\frac{\partial\alpha}{\partial x}$, as in our dimensionless variables $|\frac{\partial\alpha}{\partial x}| \leq 0.0063$).

The (scaled and non-dimensionalised) shear stresses are

$$\tau_I = \frac{r(Q^*-u)\,|Q^*-u|}{\delta\pi(1-A)^2}, \quad \tau_o = \frac{r(Q^*-Au)\,|Q^*-Au|}{(1-A)^2}, \quad \tau_w = u\,|u|\,. \tag{2.50}$$

In the case that the boundary conditions give $Q(t)$ to be constant and there are no source terms we may choose our velocity scale U such that $Q^* = 1$.

2.4 The behaviour of these functions

It is easy to see that $g_1(A)$ is an increasing function with $g_1(0) = 1$ and $g_1 \to \infty$ as $A \to 1$. We can write $g_2 = g_1(A)u + \frac{2rA}{1-A}(v-u)$, and this gives us that g_2 is positive when $u > 0$ and $v > u$ (which is typical for up-flows). We write $g_3 = -\frac{r(v-u)^2}{1-A} + \beta(1-r)\cos\alpha\frac{dh_I}{dA}$, and from this we find that $g_3 \to -\infty$ as $A \to 0, 1$ when we fix $Q_w = Au$.

As the friction factors are constant we can obtain analytical expression for the derivatives of $f(A,u)$, namely

$$\frac{\partial f}{\partial u} = -\frac{2r}{\delta\pi(1-A)}\left(\frac{1}{A} + \frac{1}{1-A}\right)|v-u|\,S_I - \frac{2rA\,|v|\,S_o}{\delta(1-A)^2} - \frac{2\,|u|\,S_w}{A}, \tag{2.51}$$

$$\begin{aligned} \frac{\partial f}{\partial A} &= \frac{r(v-u)\,|v-u|}{\delta\pi}\left(\frac{1}{1-A} + \frac{1}{A}\right)\left(\left(\frac{3}{1-A} - \frac{1}{A}\right)S_I + \frac{dS_I}{dA}\right) \\ &\quad + \frac{r\,|v|}{\delta(1-A)}\left(\frac{S_o}{1-A}(3v-2u) + v\frac{dS_o}{dA}\right) + \frac{u\,|u|}{A}\left(\frac{S_w}{A} - \frac{dS_w}{dA}\right), \end{aligned} \tag{2.52}$$

(using $\frac{\partial v}{\partial u} = \frac{v-u}{1-A}$ and $\frac{\partial v}{\partial A} = -\frac{A}{1-A}$). From these expressions it is clear that $\frac{\partial f}{\partial u} < 0$ for all A, u.

In order to gain some idea as to the size of these functions, we plot the values of g_1, g_2, g_3 at the equilibrium value as we vary α in figure 2.4

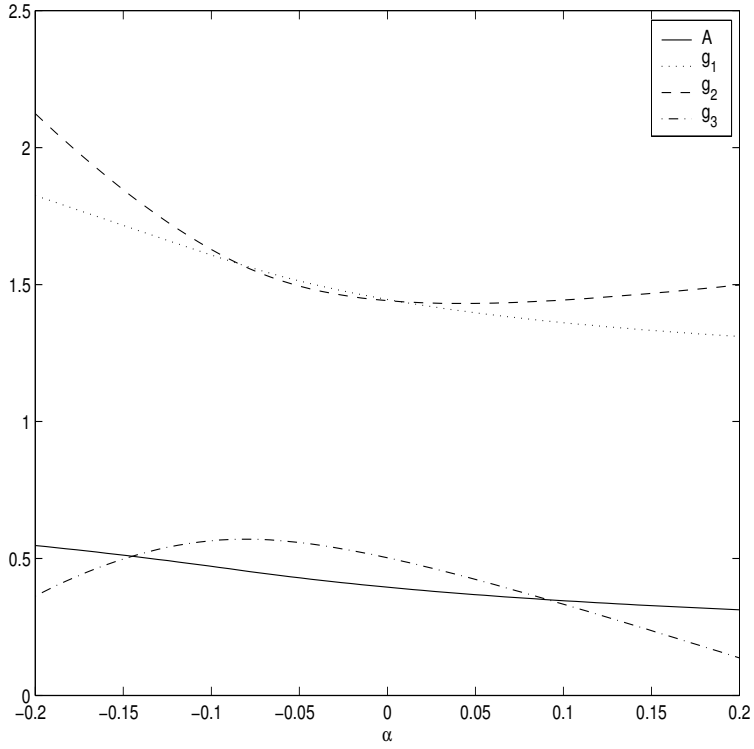

Figure 2.4: A plot of A, g_1, g_2 and g_3 at the uniform steady state as we vary α, for the Wytch farms flow parameters

2.5 Characteristics and well posedness

Equations (2.43) and (2.44) are a quasi-linear system of 2 first order pdes in two variables, and can be written in the form

$$\mathbf{A}\psi_t + \mathbf{B}\psi_x = \mathbf{c} \tag{2.53}$$

where $\psi = (A, u)^T$, and

$$\mathbf{A} = \begin{bmatrix} 1 & 0 \\ 0 & g_1 \end{bmatrix}, \qquad \mathbf{B} = \begin{bmatrix} u & A \\ g_3 & g_2 \end{bmatrix}, \qquad \mathbf{c} = \begin{bmatrix} 0 \\ f \end{bmatrix}. \tag{2.54}$$

The system has characteristics $\dot{x} = \lambda$, where $|\,\mathbf{A}\lambda - \mathbf{B}\,| = 0$, and so has characteristic speeds which are the roots of

$$g_1\lambda^2 - (ug_1 + g_2)\lambda + ug_2 - Ag_3 \;\; = \;\; 0, \tag{2.55}$$

namely

$$\lambda = \frac{1}{2g_1}\left((ug_1 + g_2) \pm \sqrt{(ug_1 - g_2)^2 + 4Ag_1g_3)}\right). \tag{2.56}$$

Hence the characteristics are both real and distinct (and so the system hyperbolic) when

$$(ug_1 - g_2)^2 \;>\; -4g_3g_1A, \tag{2.57}$$

or in terms of our original quantities

$$\frac{r(v-u)^2}{1-A} \;<\; \beta\left(1+\frac{rA}{1-A}\right)(1-r)\cos\alpha\frac{dh_I}{dA}. \tag{2.58}$$

If this inequality does not hold then the system is parabolic or elliptic, and typically not well posed as an initial value problem, as shown in [21], and we will return to this when we discuss stability of the system. When the system is hyperbolic, the two roots are of the same sign if and only if

$$\frac{g_2u - Ag_3}{g_1} \;>\; 0. \tag{2.59}$$

As it is easy to show that

$$\frac{(ug_1+g_2)}{2g_1} \;=\; \frac{u(1-A)+rAv}{(1-A)+rA}, \tag{2.60}$$

hence at least one of the characteristics is always positive for co-current flow. As with the shallow water equations, we shall call the flow *supercritical* if both characteristics are downstream (and in which case all inifinitesimal long waves propagate downstream) and *subcritical* if one of the characteristics is upstream (so infinitesimal long waves may propagate upstream and downstream). This has consequences for the type of boundary conditions necessary to obtain a well posed problem, if we have first managed (somehow) to prescribe the total mass flux at the inlet. For such a hyperbolic quasi-linear system we require the number of additional restrictions on A, u at each end of the pipe to be the same as the number of outgoing (i.e. directed into the pipe) characteristics in order to obtain a well-posed problem.

2.6 Steady state solutions

For flows not dependent on time, and with no fluid entering through the walls of the pipe, we have that

$$Au = Q_w, \qquad (1-A)v = Q_o, \quad \text{and} \quad Q_w + Q_o = Q, \tag{2.61}$$

where Q_w and Q_o are the (non dimensional) volume fluxes through the pipe, and Q is the total volume flux. Then using these expressions to eliminate u, v in (2.44) we obtain

$$L(A,x)A_x = R(A,x), \tag{2.62}$$

where

$$\begin{aligned} L(A,x) &= -\frac{Q_w g_2}{A^2} + g_3 && (2.63)\\ &= -\frac{Q_w^2}{A^3} - r\frac{Q_o^2}{(1-A)^3} + \frac{dh_I}{dA}(1-r)\beta\cos\alpha, && (2.64)\\ R(A,x) &= \frac{rS_I}{\delta}\left(\frac{1}{1-A}+\frac{1}{A}\right)\left(\frac{Q_o}{1-A}-\frac{Q_w}{A}\right)\left|\frac{Q_o}{1-A}-\frac{Q_w}{A}\right| && (2.65)\\ &\quad + \frac{rS_o}{\delta(1-A)}\frac{Q_o}{1-A}\left|\frac{Q_o}{1-A}\right| - \frac{Q_w}{A}\left|\frac{Q_w}{A}\right|\frac{S_w}{A} + \gamma(1-r)\sin\alpha. \end{aligned}$$

For a steady state it is possible to express some of the conditions found previously more concisely, and to attribute some sort of physical significance to the variables in the equations. We will define the specific energies of the two phases as

$$\begin{aligned} E_w &= p_I + \frac{1}{2}u^2 + \beta(h_I\cos\alpha + H), && (2.66)\\ E_o &= p_I + \frac{1}{2}rv^2 + r\beta(h_I\cos\alpha + H), && (2.67) \end{aligned}$$

where H is the vertical height of the midpoint of the pipe above the bottom of the well. In the absence of frictional forces on the streams we find that $\frac{d}{dx}(E_w - E_o) = 0$. However if we ignore the change in potential energy due to the deviation of the pipe from horizontal and so define

$$\begin{aligned} E'_w &= p_I + \frac{1}{2}u^2 + \beta h_I\cos\alpha, && (2.68)\\ E'_o &= p_I + \frac{1}{2}rv^2 + r\beta h_I\cos\alpha, && (2.69) \end{aligned}$$

we obtain

$$\frac{d}{dx}(E'_w - E'_o) = f, \tag{2.70}$$

so (at least in a steady state) f is a measure of the rate of transfer of energy between the streams. We can also express $L(A) = \frac{d}{dA}(E'_w - E'_o)$, so $L(A) = 0$ when the difference between the energies of the streams is at a maximum or a minimum.

2.7 Uniform steady states

A uniform steady state solution $A = \overline{A}$ is possible in a straight pipe when $R(\overline{A}) = 0$. Now, R depends on our dimensionless parameters in the combinations $\frac{\delta}{r}$, $(1-r)\gamma \sin\alpha$, and also on Q_w and Q_o. However in a steady state we can scale the velocity such that $Q = 1$. Thus for a given fluid pair the equilibrium level depends only on $\gamma \sin\alpha$ and $\xi = \frac{Q_w}{Q_o}$. The dependence of the equilibrium fluid level on these two parameters is shown in figure 2.5. We also plot $R(A)$ for various values of ξ in figure 2.6. Note that varying $\gamma \sin\alpha$ merely modifies $R(A)$ by a constant.

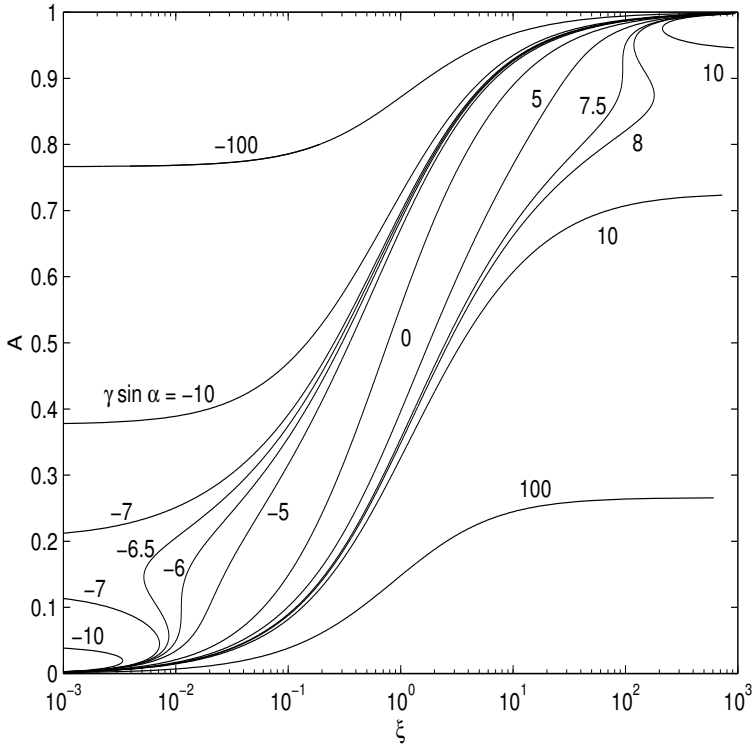

Figure 2.5: A plot showing the uniform levels of A (y-axis) for varying ξ (x-axis with logarithmic scale) and $\gamma \sin\alpha$ (contour values), for oil-water flow

It is possible to show that $R(A) \to -\infty$ as $A \to 0$ and $R(A) \to +\infty$ as $A \to 1$. It can be seen that for $\gamma \sin\alpha$ less than about -6 there are multiple (3) equilibrium steady states for some values of ξ. However this only occurs for $\xi < 0.01$ or $\xi > 0.99$. For small water cuts the water is usually dispersed in the oil phase [20], and we would expect the Multiple solutions also only occur for a very limited rage of flow rates. For counter-current flow ($Q_w < 0$ and $Q_o > 0$) then $R(A)$ is concave and strictly positive for $\sin\alpha = 0$. Thus in this case there are no equilibrium steady states unless $\gamma(1-r)\sin\alpha$ is sufficiently large and negative, in which case there are two.

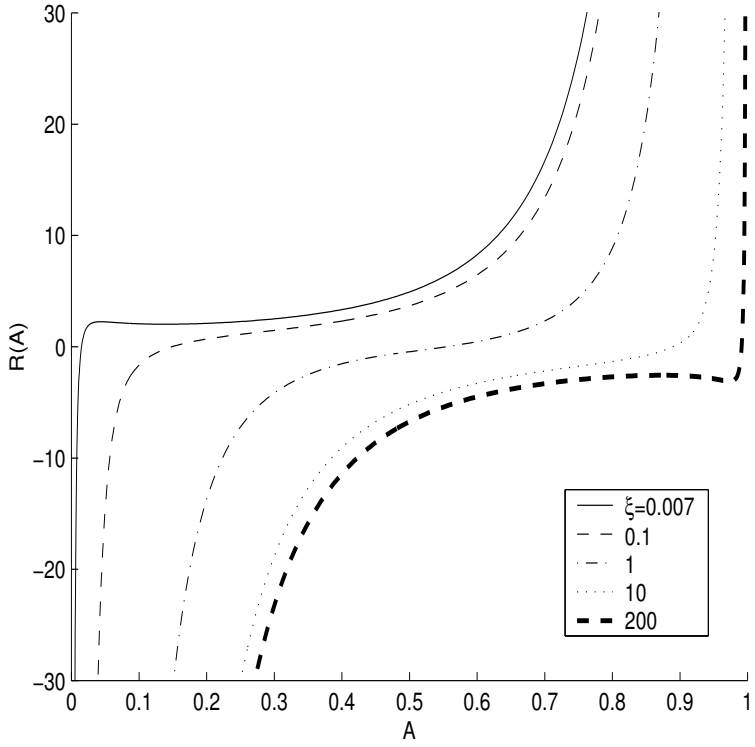

Figure 2.6: A plot of $R(A)$ against A for varying values of ξ, with $\alpha = 0$

2.8 Geometric considerations

In order to evaluate these functions numerically it is necessary to express S_w, h_I etc. in terms of A. This is done by introducing the angle θ as shown in figure 2.7, which is the angle subtended by the interface in a normal cross section at the centre of the pipe. Then by simple geometry we have

$$S_w = \frac{\theta}{2\pi}, \quad S_o = \frac{2\pi - \theta}{2\pi}, \quad S_I = \sin(\theta/2), \tag{2.71}$$

$$A = \frac{\theta - \sin\theta}{2\pi}, \quad h_I = \frac{1}{2} - \frac{\cos(\theta/2)}{2}, \quad \frac{dh_I}{dA} = \frac{\pi}{4\sin(\theta/2)}. \tag{2.72}$$

Thus as $\theta \to 0$, $A \sim \frac{\theta^3}{12\pi}$, $\frac{dh_I}{dA} \sim \frac{\pi}{2\theta}$, $S_I \sim \frac{\theta}{2}$, $S_w \sim \frac{\theta}{2\pi}$ etc., which allows us to deduce the behaviour of our functions as $A \to 0, 1$.

2.9 Behaviour of $L(A)$

The behaviour of L only depends on the dimensionless parameters ξ and $\beta\cos\alpha$. For small inclinations $\cos\alpha \simeq 1$, so $\beta\cos\alpha$ is approximately constant for a fixed total flow rate. It can be shown that $L(A) \to -\infty$ as $A \to 0, 1$. It is also simple to show

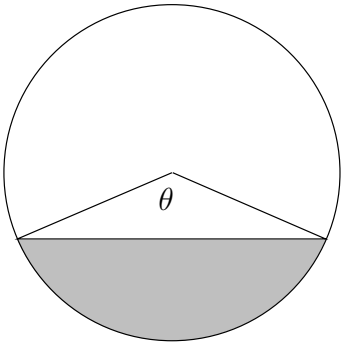

Figure 2.7: Definition of the angle θ used to numerically evaluate functions.

that $\frac{dh_I}{dA}$ takes a minimum value of $\pi/4$, and tends to ∞ as $A \to 0, 1$. Typically L is convex, and interest occurs when $L > 0$ (as here the two characteristics, if real, are in opposite directions in the steady state). This occurs for large $\beta \cos\alpha$, as can be seen in figures 2.9 and 2.9. Note that $L(A)$ has at most two roots for typical values of the flow parameters, and the location of these roots can be seen in figures 2.10 and 2.11.

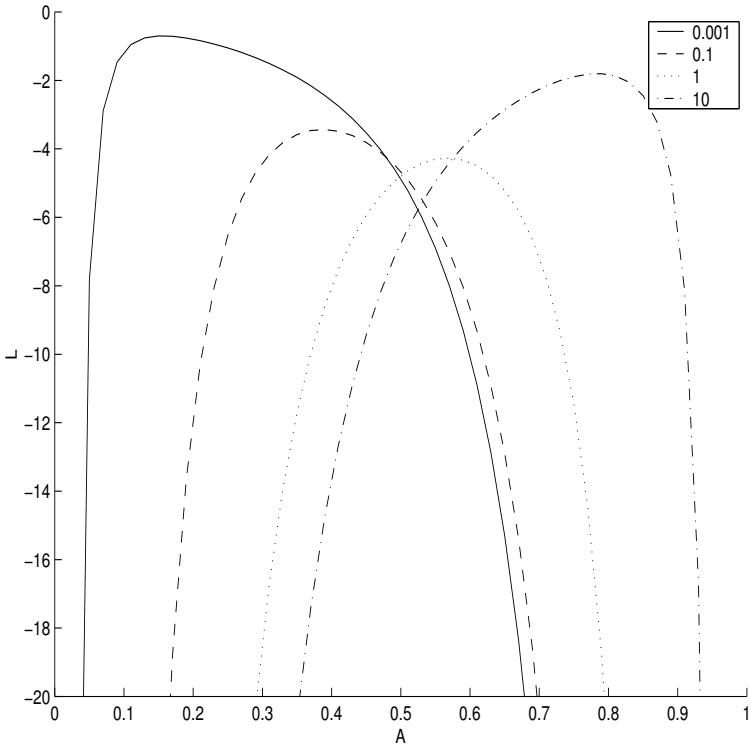

Figure 2.8: A plot of $L(A)$ against A for varying values of ξ, with $\beta \cos\alpha = 2.28$

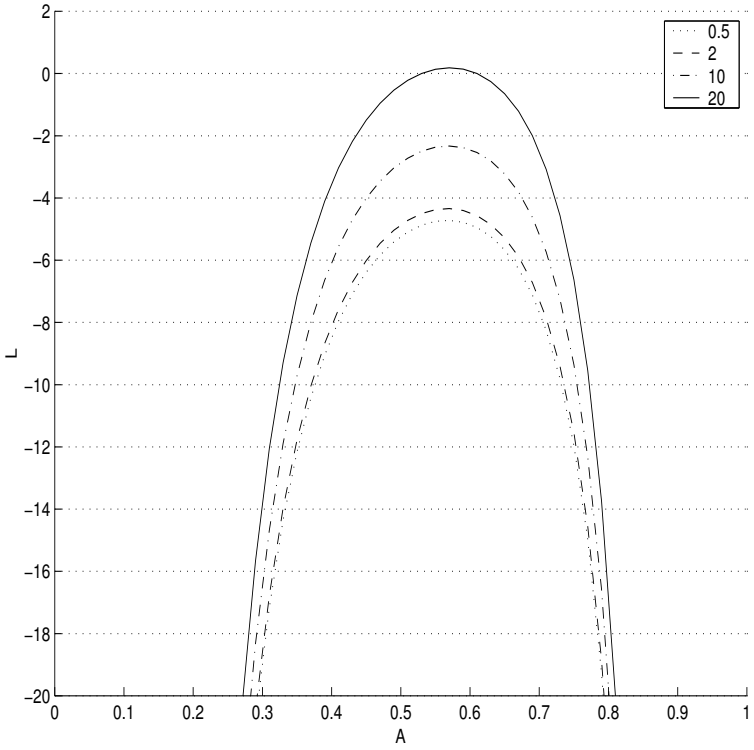

Figure 2.9: A plot of $L(A)$ against A for varying values of $\beta \cos \alpha$, with $\xi = 1$

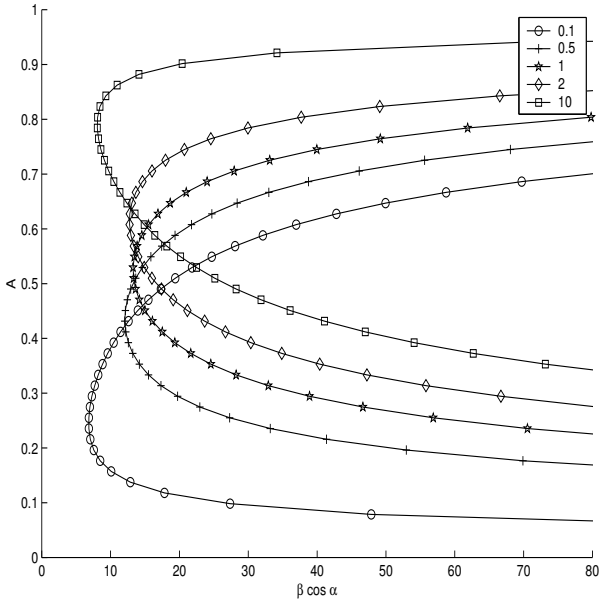

Figure 2.10: A plot showing the zeros of $L(A)$ for various values of ξ, against $\beta \cos \alpha$

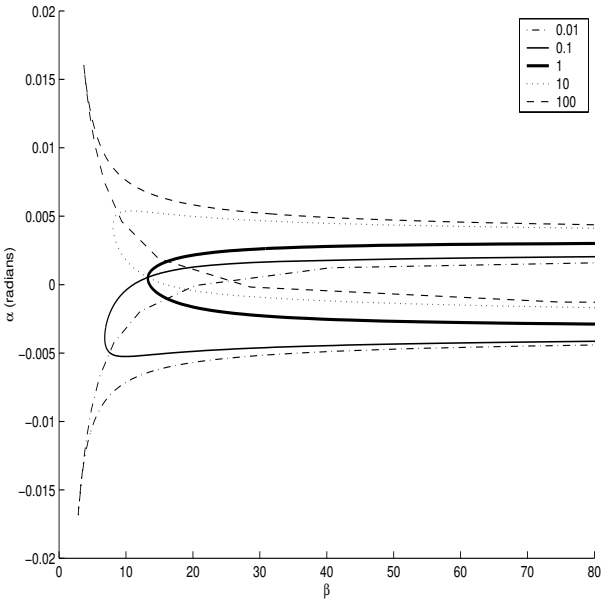

Figure 2.11: A plot showing the value of α for which the equilibrium level has $L = 0$ for various values of ξ, against β

2.10 Linear stability analysis

Wallis [47], Crowley et al. [14], Barnea and Taitel [6] and [7], Brauner and Moalem Marron [32] and Trallero [45] all examine the stability of uniform steady-state stratified flows using a two fluid model which is basically the same as ours. We will roughly follow the development of Wallis.

For a uniform basic flow $A = \overline{A}$, $u = \overline{u}$ the linearised equations governing the evolution of small perturbations $A = \overline{A} + A$, $u = \overline{u} + u'$ are

$$A'_t + \overline{A}u'_x + \overline{u}A'_x = 0, \tag{2.73}$$

$$g_1 u'_t + g_2 u'_x + g_3 A'_x = f_A A' + f_u u'. \tag{2.74}$$

Such a steady state is crudely said to be *stable* if any sufficiently small amplitude perturbation remains small for all time, otherwise the steady state is *unstable*. Provided $\overline{A} \neq 0$ we can obtain a linear second order pde for A, as in [47] and [50], by differentiating (2.74) with respect to x and then using (2.73) to eliminate u, to give

$$(g_3 - \frac{g_2\overline{u}}{\overline{A}})A_{xx} - \frac{1}{\overline{A}}(g_2 + \overline{u}g_1)A_{xt} - \frac{g_1}{\overline{A}}A_{tt} = (f_A - \frac{f_u\overline{u}}{\overline{A}})A_x - \frac{f_u A_t}{\overline{A}}. \tag{2.75}$$

It is trivial to show that this can be written in the form

$$G\left(\frac{\partial}{\partial t} + \lambda_1\frac{\partial}{\partial x}\right)\left(\frac{\partial}{\partial t} + \lambda_2\frac{\partial}{\partial x}\right)A = \left(\frac{\partial}{\partial t} + V\frac{\partial}{\partial x}\right)A, \tag{2.76}$$

where λ_1 and λ_2 are the characteristic speeds given by equation 2.56 and $V = \overline{u} - \frac{\overline{A} f_A}{f_u}$ given by is the *kinematic wave speed*, whose significance will be discussed later. We will shortly show that

$$G = -\frac{g_1}{f_u} > 0 \tag{2.77}$$

is necessary for stability.

For temporal stability, consider normal modes $A' = \hat{A} e^{ikx+\sigma t}$. Then non-trivial solutions are possible provided σ satisfies

$$G\sigma^2 + [G(\lambda_1 + \lambda_2)ik + 1]\sigma + [ikV - G\lambda_1\lambda_2 k^2] = 0, \tag{2.78}$$

which has solutions given by

$$\sigma = \frac{1}{2G}\left(-G(\lambda_1 + \lambda_2)ik\sigma - 1 \pm \sqrt{1 - k^2G^2(\lambda_2 - \lambda_1)^2 + 2ikG(\lambda_1 + \lambda_2) - 4GikV}\right). \tag{2.79}$$

Such a mode is stable when if $\Re(\sigma) < 0$, neutrally stable if $\Re(\sigma) = 0$ and unstable when $\Re(\sigma) > 0$. Unstable normal modes are amplified, whereas stable normal modes diminish in amplitude (in the linearised problem). Putting k=0 into this expression we see that $G > 0$ is a necessary condition for stability, and as $g_1 > 0$ always this is equivalent to $f_u < 0$. Now, if

$$p + iq = \sqrt{1 - k^2G^2(\lambda_2 - \lambda_1)^2 + 2ikG(\lambda_1 + \lambda_2) - 4GikV}, \tag{2.80}$$

then the real part of σ is positive only when $p > 1$. We now consider the cases when the characteristic speeds are real and complex separately.

In the case when the characteristics are real (and so the linear system comprising equations (2.43) and (2.44) is hyperbolic) suppose $\lambda_1 < \lambda_2$. Then we find that

$$p^2 - q^2 = 1 - k^2G^2(\lambda_1 - \lambda_2)^2, \tag{2.81}$$

$$pq = Gk[(\lambda_1 + \lambda_2) - 2V], \tag{2.82}$$

so p satisfies

$$p^2 - \frac{G^2k^2[(\lambda_1 + \lambda_2) - 2V]^2}{p^2} = 1 - k^2G^2(\lambda_1 - \lambda_2)^2. \tag{2.83}$$

The left hand side of this equation is a strictly increasing function of p, so p is a function of k. For simplicity, writing $\psi = p^2$, $l = k^2$, $a = Gk[(\lambda_1 + \lambda_2) - 2V]b = kG(\lambda_1 - \lambda_2)$, we have

$$\psi - \frac{la^2}{\psi} = 1 - lb^2, \tag{2.84}$$

and as $\psi(0) = 1$ and $\psi(\infty) = \frac{a^2}{b^2}$ it is simple to show that ψ is a monotone function (increasing or decreasing depending on whether $\frac{a^2}{b^2}$ is less than or more than one), and so has bound $\max\left(\frac{a^2}{b^2}, 1\right)$. Thus instability occurs when $a^2 > b^2$, which is the case when V lies outside $[\lambda_1, \lambda_2]$, as noted in [50]. In this case the maximal amplification factor is for short waves ($k \to \infty$), for which

$$\sigma = \frac{1}{2G}\left(\frac{|\,\lambda_1 + \lambda_2 - 2V\,|}{|\,\lambda_2 - \lambda_1\,|} - 1\right). \tag{2.85}$$

In the case when the characteristics are complex the linear system is elliptic, and $\lambda_1 = \overline{\lambda_2}$. Thus $(\lambda_2 - \lambda_1) = 2\Im(\lambda_1)$, $(\lambda_1 + \lambda_2) = 2\Re(\lambda_1)$ and as before we obtain

$$p^2 - \frac{4k^2G^2[\Re(\lambda_1) - V]^2}{p^2} = 1 + 4k^2G^2\Im(\lambda_1)^2, \tag{2.86}$$

or

$$\psi - \frac{la^2}{\psi} = 1 + lb^2, \tag{2.87}$$

(where now $b = i(\lambda_1 - \lambda_2)kG$ and in this case $\psi(0) = 1$ and $\psi \to \infty$ as $k \to \infty$. Thus the amplifiction factor of small wavelength modes grows without bound (a Helmholtz instability).

Clearly the first condition (V is outside the range $[\lambda_1, \lambda_2]$) must occur before the second as the characteristics merge ($\lambda_1 = \lambda_2$) before becoming complex. The first condition can be expressed in terms of the quantities g_1, f etc. to give

$$g_1(\frac{g_2}{\overline{u}} - g_1)\overline{u}\ f_A\,|\,f_u\,| - g_1^2\overline{A}f_A^2 > -g_1g_3\,|\,f_u\,|^2\ . \tag{2.88}$$

as a necessary condition for stability. This can be expanded in terms of the original flow quantities to give

$$2r(v-u)\psi - (1 - A + rA)A\psi^2 > r(v-u)^2 - \beta(1-r)\cos\alpha\frac{dh_I}{dA}(1-A), \tag{2.89}$$

where $\psi = \frac{f_A}{|f_u|}$.

These conditions are commonly referred to as the *viscous Kelvin-Helmholtz (VKH)* and *inviscid Kelvin-Helmholtz (IKH)* criteria, in an analogy with the condition for instability of parallel shear flow obtained by solving Laplace's equation in both fluids, as for instance in [17]. There is a significant difference in the stability behaviour as in the case considered there sufficiently small wavelength waves are always unstable. However we have made an assumption that the pressure distribution is hydrostatic in each cross section, and this is only valid for large wavenumber k. It must be noted that the introduction of surface tension or a sheltering coefficient to the problem will

modify this analysis, but only in the case of large k, and when the state is unstable it is unstable for all $k \neq 0$. Hence such terms do not alter the overall stability of the steady state.

When the IKH instability occurs it results in the problem being ill-posed as an initial value problem (A, u given on $t = 0$) as the amplification factors for short wavelength waves are unbounded, so arbitrarly small solutions become large in a finite time, and the solution does not depend continuously on the initial data.

Clearly these results hold for any system for which the equations govening the evolution of small perturbations can be written in the same form as equation (2.76).

2.11 Properties of steady states

For any given choice of pipe inclination and flow rates of the two fluids there is a unique stratified (co-current) steady state (provided the water cut is between 1% and 99%), although this may not be realisable in practice through being unstable. The well-posedness and linear stability, and direction of the characteristics of a uniform steady state all depend on the values of g_1, g_2 and g_3 at the steady state. In addition the linear stability of the steady state depends on f_u and f_A. Hence they depend on the total volume flux (and so when we scale $Q = 1$ this varies β and γ).

In figure 2.12 we plot the equilibrium liquid level against water cut Q_w (where $Q_o = 1 - Q_w$) and pipe angle α for a variety of total flow rates.The diagrams show the boundaries of ill-posedness and linear stability for the solutions, and also the direction of the characteristics (typically the flow is supercritical). A very similar stability analysis (with non-constant friction factors) was conducted in [32]. There the linear stability condition was deemed to denote the transition from stratified to wavy-stratified flow, and the ill-posedness condition denoted the transition to a dispersed regime. However other authors such as [20] have claimed that the neutral curve of the linear stability condition denotes the transition from smooth stratified flow to stratified flow with a mixing region between the layers.

In summary from figure 2.12 we can see that

1. For a fixed angle, the hold-up increases with the water cut.

2. For a fixed water cut the hold up decreases with α, and so is greater uphill than downhill. This effect is more pronounced at low flow rates (which corresponds to a larger value of β).

3. The flow is typically linearly stable for horizontal flow, but becomes unstable when α is roughly ± 0.02 radians $\simeq \pm 1^\circ$ (this depends on the flow rates of the two fluids)

This appears to be in general agreement with the experimental results, except that there is a discrepancy at low flow rates, where in experiments the flow appears to be generally stable, even for moderately large angles of inclination ($\pm 5^\circ$). The choice of frictional terms may be the cause of this, although it could also be affected by the assumption that $D = 1$ in both phases [32]. The stability and the sub/supercriticality of the uniform steady states can be seen for fixed α and varying Q_w and Q_o in figures 2.14 to 2.18. In these plots Q_w and Q_o vary between 0.01 and 10, which in dimensional terms corresponds to flow rates of 64 to 64000 barrels per day of each phase. For the region of parameters covered by these plots there is only one equilibrium solution.

2.12 Boundary Conditions

The issue of the actual boundary conditions is rather vexed. In Schlumberger's flow loop the fluids are pumped into the main pipe via smaller pipes on the side of the large pipe, and so we can prescribe the inlet mass fluxes of the two fluids (possibly be regulating the pressure in the pipes through which the fluids are introduced). However, if we prescribe the pressure in both fluids at the inlet, and the hydrostatic pressure assumption holds at the inlet, then the interface height is known. Thus it appears to be the case that we can only prescribe two of Q_o, Q_w and A independently at the inlet to the pipe. Experiments have been performed studying the transition to slugging in air-water flows in [52] where the two fluids are introduced on either side of a splitter plate, and so it appears that A is being prescribed at the inlet. However there it was found that if a value of A is just chosen arbitrarily then slugging tends to develop at the inlet of the pipe, rather than at a distance of about $50d$ from the inlet. Hence it appears to be the case that we cannot physically prescribe so many boundary conditions at the inlet (where the stream is typically supercritical), but in order to have a well defined problem we will assume that we are able to prescribe both mass fluxes and the void fraction at the inlet. At the outlet typically we let the flow flow out into the atmosphere - thus p_I is atmospheric pressure at this point. We will assume that there is no restriction on the pressure at the inlet (so the system and boundary conditions can then be considered to be hyperbolic). Down-hole however the situation is more confused. However we will assume that the pressure drop over the well is a constant. In actual fact there is a pump in the well, and the pressure at

which the fluids enter the pipe will depend on the flow in the reservoir and through the perforations, but the situation is unclear.

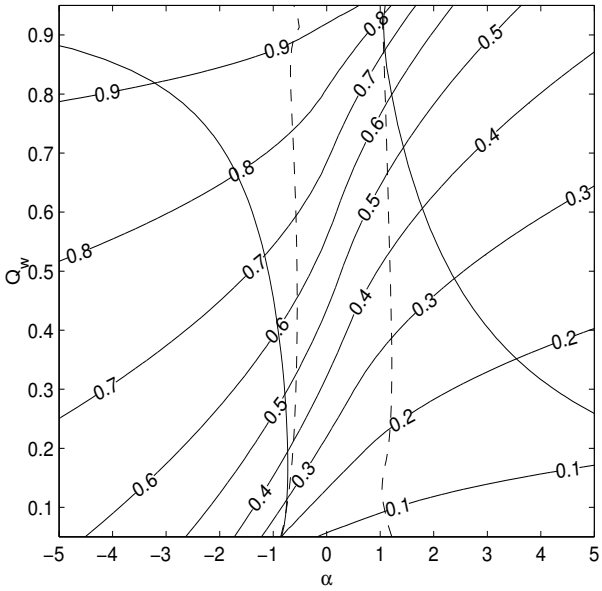

(a) $\beta = 2.3$ which corresponds to a mean flow rate of 0.78ms^{-1} or 6400bpd

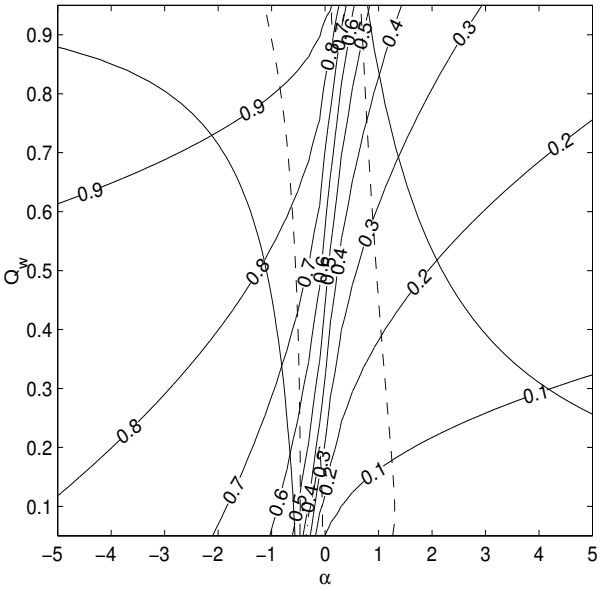

(b) $\beta = 10$ which corresponds to a mean flow rate of 0.37ms^{-1} or 3100bpd

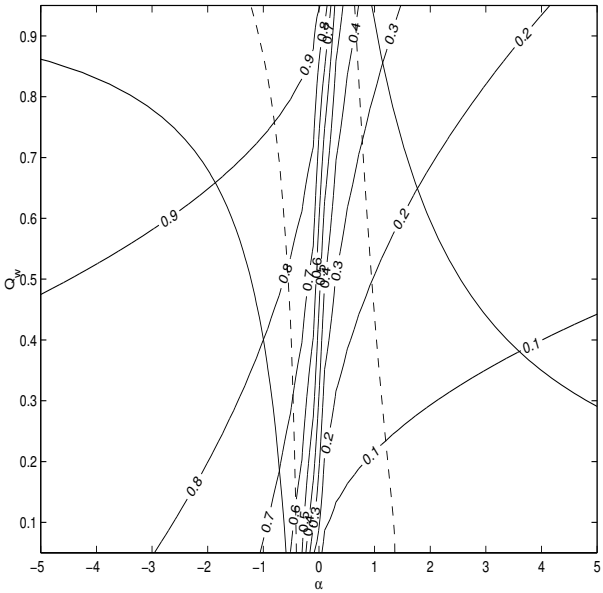

(c) $\beta = 20$ which corresponds to a mean flow rate of 0.26ms^{-1} or 2200bpd

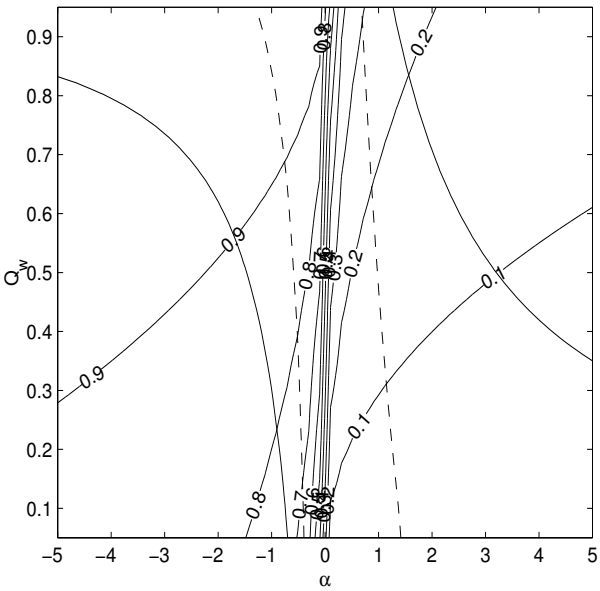

(d) $\beta = 40$ which corresponds to a mean flow rate of 0.19ms^{-1} or 1500bpd

Figure 2.12: Diagrams showing neutral stability and equilibrium flow level height for a number of different flow rates.The dotted line is the linear stability boundary, and the solid line is the line across which the system becomes ill-posed. The numbered curves denote the value of A at equilibrium. Here α is measured in degrees

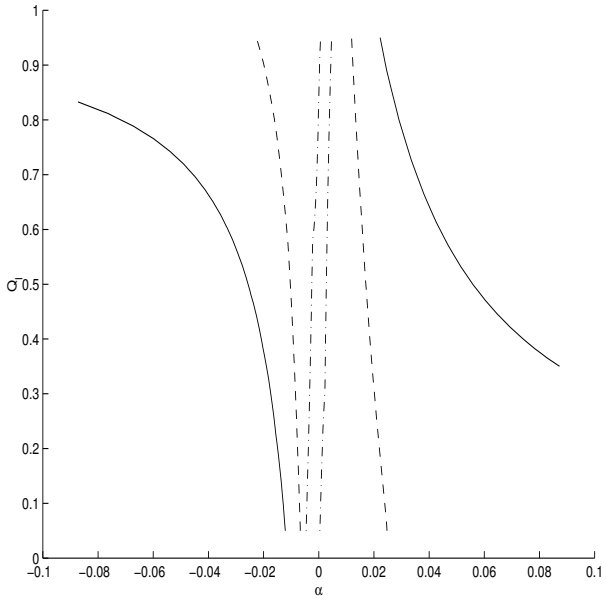

Figure 2.13: As in figure 2.12 but showing where the flow is subcritical (in between the two dash-doted lines) for $\beta = 40$

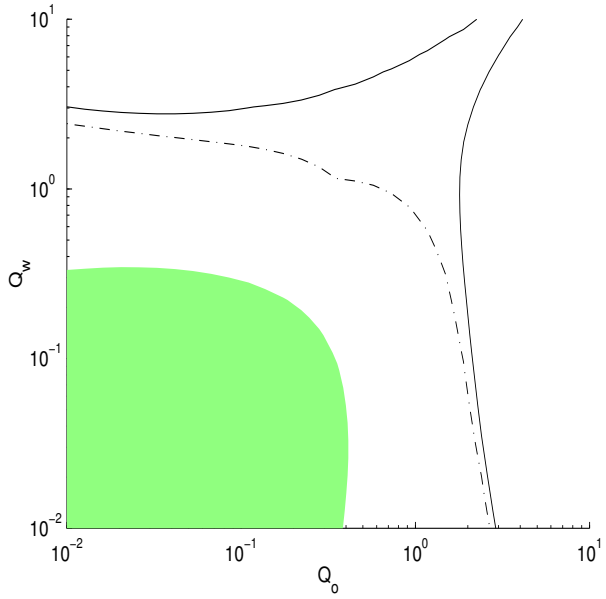

Figure 2.14: This plot shows the criticality (subcritical in shaded region), linear stability (dotted line, stable in bottom left) and well-posedness (solid line, well posed in bottom left) for oil-water flow in a straight horizontal pipe, in terms of the non-dimensional volume fluxes Q_w and Q_o

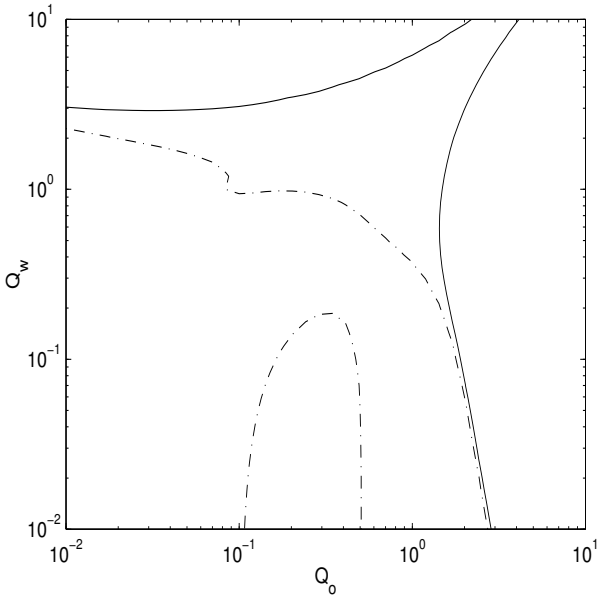

Figure 2.15: As figure 2.14 but for a 0.5° upflow ($\alpha = -0.0087$)

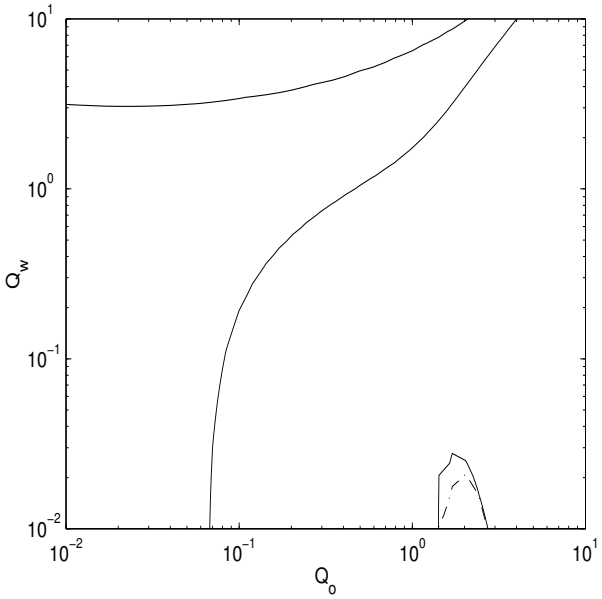

Figure 2.16: As figure 2.14 but for a 2° upflow ($\alpha = -0.035$)

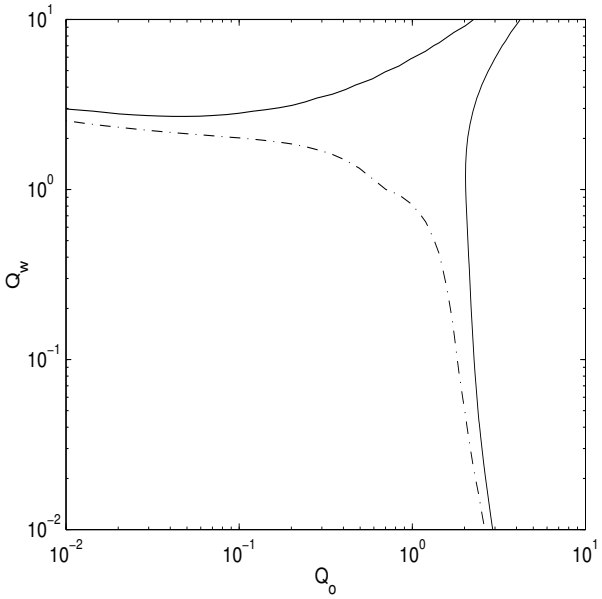

Figure 2.17: As figure 2.14 but for a 0.5° downflow ($\alpha = 0.0087$)

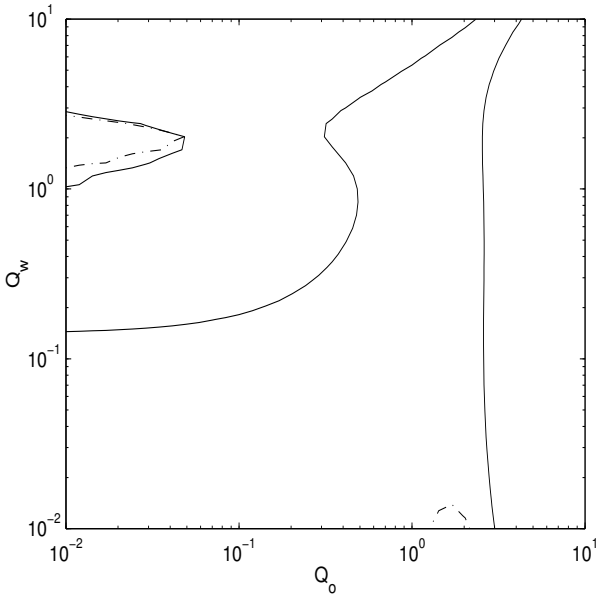

Figure 2.18: As figure 2.14 but for a 2° downflow ($\alpha = 0.035$)

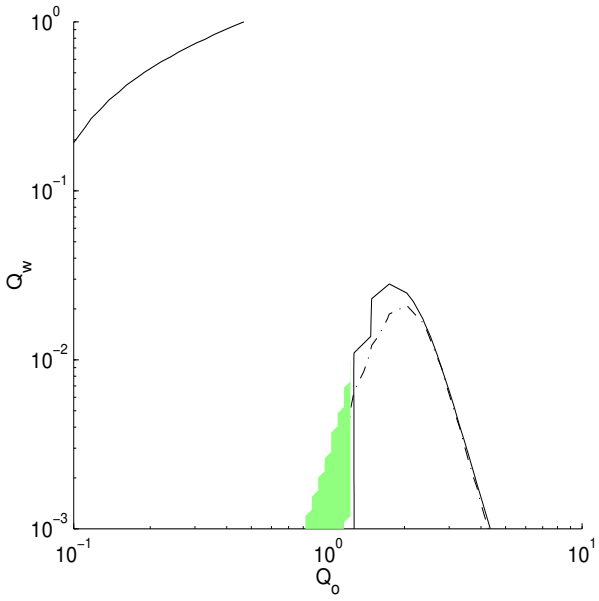

Figure 2.19: As figure 2.16 but showing the region for which multiple equilibria occur (shaded), and with different scales. However this only occurs for unrealistically low water flow-rates (less than 50 barrels per day in a total flow of about 6000 barrels per day), and the flow is unlikely to be stratified.

Chapter 3

Shocks and Roll Waves

3.1 Travelling wave solutions

The linear stability analysis in section (2.10) only governs the evolution of a perturbation while it is small, and it is natural to ask what the unstable modes evolve into as they become finite in amplitude. It is plausible that travelling waves occur, as occurs at the instability for single phase flow in a channel, studied by Dressler [18]. Let $\xi = x - ct$ be the coordinate for a wave of constant form travelling in the direction of increasing x with speed c, so $A = A(\xi)$ and $u = u(\xi)$. Then the equations (2.43) and (2.44) become (with $' = \frac{d}{d\xi}$)

$$-cA' + (Au)' = 0, \tag{3.1}$$

$$-cg_1u' + g_2u' + g_3A' = f, \tag{3.2}$$

and on integrating (3.2) and (3.2) we find that the specific discharges P_w, P_o are constant, with

$$P_w = A(u-c), \qquad P_o = (1-A)(v-c), \qquad Q = P_w + P_o + c, \tag{3.3}$$

Eliminating u in (3.2) gives

$$\left(-\frac{P_w}{A^2}(g_2 - cg_1) + g_3\right)A' = f(A, \frac{P_w}{A} + c), \tag{3.4}$$

or

$$L_T(A)A' = R_T(A), \tag{3.5}$$

where now

$$L_T(A) = -\frac{P_w^2}{A^3} - r\frac{P_o^2}{(1-A)^3} + \beta(1-r)\cos\alpha\frac{dh_I}{dA}, \tag{3.6}$$

$$R_T(A) = f(A, \frac{P_w}{A} + c), \tag{3.7}$$

and f is as in equation (2.44). Equation (3.5) is a first order autonomous ODE for A, and so all continuous solutions are monotone. In particular the equation has no continuous periodic solutions. As in Dressler [18] we will attempt to construct periodic *roll-wave* solutions by joining monotone continuous solutions of (3.5) with finite jump discontinuities.

3.2 Jump conditions

The system of equations (2.43) and (2.44) is hyperbolic, and so we would expect that for some initial data the solution will become multi-valued when the characteristics of the equation intersect. When this occurs we normally assume that the solution becomes discontinuous at this point, with smooth solutions to either side of a finite discontinuity in A, u. If we wish to determine the evolution of the solution after this time the speed of the shock needs to depend on the flow properties on either side of the shock. Furthermore such shocks are necessary to construct the desired roll wave solutions.

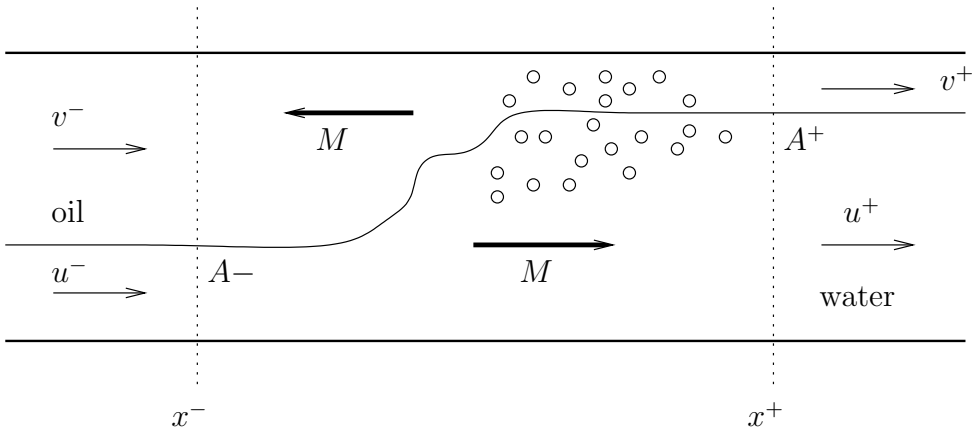

Figure 3.1: Schematic diagram of a hydraulic jump or bore in liquid-liquid flow.

We will assume that $x_+ - x_-$ is sufficiently small so that the effects of gravity and friction at the walls are negligible. If this is the case then for a shock moving at a steady rate we may consider the problem in a frame in which the shock is stationary. We will also assume that the proportion of fluid *entrained* (mixed from one phase into the other) is negligible and that the flow is fully developed outside of the shock region, so our simple model is valid except in the shock. Considering conservation of mass for each phase across the shock give us that

$$[Au] = [(1 - A)v] = 0, \tag{3.8}$$

where [] denotes the change in a quantity from $x = x^-$ to $x = x^+$. Thus we have that the mass fluxes $Q_w = Au$ and $Q_o = (1 - A)v$ are continuous across the jump. Let F denote the sum of forces acting in the direction of increasing x on the lower layer due to the effect of the interfacial friction and pressure. Then a corresponding force $-F$ acts on the upper layer. Considering the rate of change of momentum for the water layer gives

$$[A_c(p_w A + \rho_w A u^2)] \quad = \quad F, \tag{3.9}$$

where p_w is the mean pressure in the lower layer, and from equation (2.11) $p_w = p_I + \rho_w g h_w \cos\alpha$. Thus in terms of our dimensionless quantities we obtain

$$[p_I A + A(u^2 + \beta h_w \cos\alpha)] \quad = \quad F, \tag{3.10}$$

where F has been scaled with $\rho_w A_c U^2$. Similar considerations for the oil phase give

$$[p_I(1 - A) + r(1 - A)(v^2 + \beta h_o \cos\alpha)] \quad = \quad -F, \tag{3.11}$$

These two equations may be added to eliminate F and we obtain

$$[p_I + (Au^2 + \beta A h_w \cos\alpha) + r((1 - A)v^2 + \beta(1 - A)h_o \cos\alpha)] = 0. \tag{3.12}$$

However, once the equations of motion have been converted into shallow water form (equations (2.43) and (2.44)) p_I does not appear explicitly, and so this condition gives no restriction on the jump. As with the shallow water equations we would expect that, for given values of $A-$ and $u-$ there exist unique values of $A+$ and $A-$. These are obtained in the equations for flow in a open conduit by considering conservation of mass and momentum across the shock, as shown in [41]. This discrepancy was first noted by Benton [9] for two-dimensional flow in a channel (both with a free surface and a closed lid). In order to resolve this problem we need to either determine another conserved quantity across the shock, or parametrise the momentum transfer between the phases.

Most authors have only studied the two-dimensional case, either with a closed lid or an open free surface, as this problem has applications to hydraulic jumps in between two layers in the atmosphere, often induced by variations in the topography of the ground (mountains etc.) Commonly in such applications there is a small density difference in between the two phases, and so the Boussinesq approximation may be made where the density difference is ignored except in the body force terms. The first attempts to resolve this situation by [29], [53], and [30] assumed that the pressure at

the shock front is hydrostatic, with the pressure at the interface the average of that on the two sides. This does give another relation for the shock, and apart from the obvious assumptions made it is not particularly satisfactory as it can give up to 3 solutions for $A+$ and allows the energy per unit volume of both streams to increase across the shock. Boudlal and Dyment [10] studied the case of infinitesimal jumps in a pipe, although they made the basic assumption that the interfacial momentum transfer was, to first order in the height of the jump, due to hydrostatic pressure.

Some authors have required that the energy per unit volume of either the contracting phase [51], or the expanding phase [25], is conserved across the shock. This is equivalent to asserting that

$$0 = [\beta h_I \cos\alpha + u^2/2 + p_w], \tag{3.13}$$

in the first case, or a similar equation when the energy of the other phase is conserved. Other authors [3] assert there is no energy loss in both phases for a weak shock, which occurs when $[A]$ is small. This agrees reasonably well with the other ideas, as [24] and [10] show that their assumptions give energy losses of order $O([A]^3)$ in each phase for a weak shock.

Drew and Passman [19] suggest manipulating equations (2.24) and (2.25) to obtain an equation without p_I in conservation form, but this is merely equivalent to assuming conservation of energy of one of the phases. Other authors [48] and [27] assume that $E_o - E_w$ (as introduced in section 2.6) is conserved. We will choose this quantity to be constant by introducing an eddy viscosity term into the equations, as in Jiang and Smith [24]. This was also considered by Armi [3] to be a good approximation to his criterion for a weak shock. One condition that certainly must be satisfied is that the shock dissipates (mechanical) energy converting it into heat etc. via turbulent stresses, and this is the case when

$$Q_w[E_w] + Q_o[E_o] \leq 0. \tag{3.14}$$

3.3 Eddy viscosity and shock structure

In our model the Reynolds Stresses in the direction of the flow have been approximated by our friction factor terms. As in Needham and Merkin [34] we introduce an eddy viscosity term to account for the Reynolds stresses normal to the flow. The exact form for such a term is unknown for our problem, and it may make a difference to the quantity conserved across the across the shock, as seen in Merkin and Needham

[31]. However for a weak shock we expect that such differences are negligible. Jiang and Smith [24] are able to justify their choice of viscosity term for a two dimensional problem, but this introduces numerical difficulties, and so we will assume that the eddy viscosity term is of the form ϵA_{xx}. Then our profile equation (3.5) becomes

$$L_T(A)A_x = R_T(A) - \epsilon A_{xx}. \tag{3.15}$$

In order to consider the inner shock problem rescale $x = \frac{x^- + x^+}{2} + \epsilon\eta$. Then to first order in ϵ we obtain the inner problem

$$L_T(A)A_\eta = -A_{\eta\eta}. \tag{3.16}$$

When the outer solution has finite derivatives at $x = x^-$ and $x = x^+$ such a solution must satisfy the boundary conditions $A \to A^-$ as $\eta \to -\infty$, $A \to A^-$ as $\eta \to \infty$ in order to match satisfactorily with the outer solution. As $L = \frac{dE_w - E_o}{dA}$ in such a steady state hence equation 3.16 integrates to give

$$E_w(A) - E_o(A) = A_\eta + \text{const}, \tag{3.17}$$

and as $A_\eta \to 0$ as $\eta \to \pm\infty$ we see that

$$[E_w - E_o] = 0. \tag{3.18}$$

We also find that $L_T(A_c) = 0$ for some A_c between A^- and A^+ (as $L_T = \frac{d}{dA}(E_w - E_o)$), so (at least for a weak shock) L must change sign across the shock, and so the sign of one of the characteristic speeds must change. In order for such a shock to be a stable solution of the hyperbolic system we require that this characteristic speed changes from being positive to being negative as we cross the shock. If it changes instead from negaitive to positive then we obtain an expansion fan in this characteristic, and the solution will become continuous.

3.3.1 Roll wave parameters

As the profile is governed by a first order ODE the wavelength and form of the continuous portion of the roll wave is uniquely determined by the values of A at the two end points, along with the wave speed c and the two specific discharges P_w and P_o. As can be seen from the previous section, shocks between $A = A^-$ and $A = A^+$ are only possible if there is some A_c such that $L_T(A_c) = 0$. However in the solution of equation (3.5) for the continuous section of the roll wave clearly A' will blow up unless $R_T(A_c) = 0$ as well at this point. This gives us a relation between the values

of P_w, P_o and c. Although in such a travelling wave solution the volume fluxes past a point will in general be periodic in time, it is plausible that we may prescribe the average over a period (or equivalently a wavelength) $\overline{Q_w}$ and $\overline{Q_o}$ of these quantities. Thus we have two further restrictions on the flow parameters

$$\overline{Q_w} = P_w + c\frac{\int_0^l A}{l}, \tag{3.19}$$

$$\overline{Q_o} = P_o + c\frac{\int_0^l (1-A)}{l}. \tag{3.20}$$

where l is the wavelength of the roll-wave. P_w and P_o are not independent as $P_w + P_o + c = Q$, and Q is constant in such a solution. The jump condition across the shock $L_T(A^-) = L_T(A^+)$ gives us another restriction on the flow quantities, and so we obtain a one-parameter family of roll waves.

3.4 Infinitesimal Roll Waves

In order to construct roll-wave solutions which are small perturbations of a steady state solution $f(\overline{A}, \overline{u}) = 0$ it is simpler to choose the parameters defining the roll wave as the holdup and velocity at the critical height, A_c and u_c, the holdup at the crest of the wave A_+, the wave speed c and the discharge of water P_w. We can in general express $L_T(A)$ as

$$L_T(A) = -\frac{(u-c)}{A}(g_2 - cg_1) + g_3, \tag{3.21}$$

by substituting $P_w = A(u-c)$ into equation 3.7. Thus the condition that $L = 0$ when $A = A_c$, $u = u_c$ gives us that

$$-c^2 g_1 + c(g_2 + ug_1) - (ug_2 - g_3 A) = 0, \tag{3.22}$$

and so c is one of the characteristic speeds λ_1 or λ_2 of the system at the steady state. Hence $c = \lambda_1$ or $c = \lambda_2$. Once we have chosen c, P_w is given by $P_w = A_c(u_c - c)$. We may then construct a one parameter family of roll waves by a choice of A^+, as then A^- is given by the condition (3.18). For A^+ and A^- near A_c we may linearise the profile equation (3.5) to give

$$\frac{dL_T}{dA}(A_c)(A - A_c)A' = \frac{dR_T}{dA}(A_c)(A - A_c), \tag{3.23}$$

and so

$$A' = \frac{\frac{dR_T}{dA}(A_c)}{\frac{dL_T}{dA}(A_c)}, \tag{3.24}$$

Now

$$\frac{dR_T}{dA} = \frac{d}{dA}\left(f(A, \frac{P_w}{A} + c)\right) = f_A + \frac{|f_u| P_w}{A^2}, \tag{3.25}$$

and so

$$\frac{dR_T}{dA}(A_c) = \left(\left(\frac{A_c f_A}{|f_u|} + u\right) - c\right)\frac{|f_u|}{A_c} = \frac{|f_u|}{A_c}(V - c), \tag{3.26}$$

where V is the speed of continuity waves. It is also possible to express L_T in the form

$$L_T(A) = -\frac{P_w^2}{A^3} - r\frac{P_o^2}{(1-A)^3} + \beta(1-r)\cos\alpha\frac{dh_I}{dA}, \tag{3.27}$$

and so $L_T(A)$ is of a similar form to $L(A)$ in the case of steady state solutions, namely that it will have precisely two roots $0 < A_1 < A_2 < 1$, with $\frac{dL_T}{dA}(A_1) > 0$ and $\frac{dL_T}{dA}(A_2) < 0$. In co-current flow when $c = \lambda_1$ the characteristic speeds (in the moving frame of reference) are both positive when $L < 0$, and one is positive when $L > 0$. Hence in order for a roll wave to be possible L must be positive to the left of the critical point and negative to the right of the critical point. Therefore we require that $R_T < 0$, which is the case only when $V < \lambda_1$. A similar analysis may be performed when $c = \lambda_2$, and in this case we find that L must increase across the critical point, and this can occur only if $R_T > 0$, which corresponds to $V > \lambda_2$. Hence small amplitude roll waves can only occur when V is outside the range of λ_1 and λ_2. However this corresponds to linear instability of the steady state as in section 2.10. For these roll waves the mean flow rate may not be exactly equal to that of the original steady state, but by taking the amplitude sufficiently small we can make the difference as small as we like.

These roll waves are possible only when the original flow is unstable, and it seems plausible that this corresponds to a *Hopf bifurcation* of the uniform steady state, as in Needham and Merkin [34] for flow in an open inclined channel.

Chapter 4

Terrain slugging at low flow rates

4.1 Initial conjecture

Initial studies by Schlumberger suggested that the slugging at low flow rates was due to the fact that at low flow rates (approximately 2200 barrels per day) the function $L(A, x)$ has a pair of zeros, and as we vary the pipe inclination the position of the uniform equilibrium solution moves so the flow is subcritical in the near horizontal sections and supercritical in the slightly deviated sections. For small inclinations the values of A for which $L = 0$ do not vary greatly with x. If such zeros are present there is no steady state flow for a pipe with slowly varying inclination (for which we expect that the steady state solution will be approximately the uniform equilibrium level as the x derivatives of the solution are small). As in the case for roll wave solutions a continuous steady state solution may only pass through the critical values if $R(A, x)$ is zero. However it is not possible for this to occur when A passes through the larger of the two zeros of $L(A, x)$ when A is increasing, as $\frac{dR}{dA}$ is always positive (provided the water cut is between 1% and 99%). Furthermore, it is not possible to have a stable hydraulic jump increasing across this value of A, as the flow is subcritical upstream and supercritical downstream. Hence some sort of time dependent behaviour is expected.

4.2 Density wave oscillations

However this effect occurs at total flow rates which are much lower than those observed in the slugging wells. We conjectured instead that movement of the position at which the flow became linearly unstable would vary as the proportion of water cut varied, and this would cause an instability of the steady state, in a similar manner to the Ledinegg instability studied in [22]. However numerical calculations (Figure 4.3)

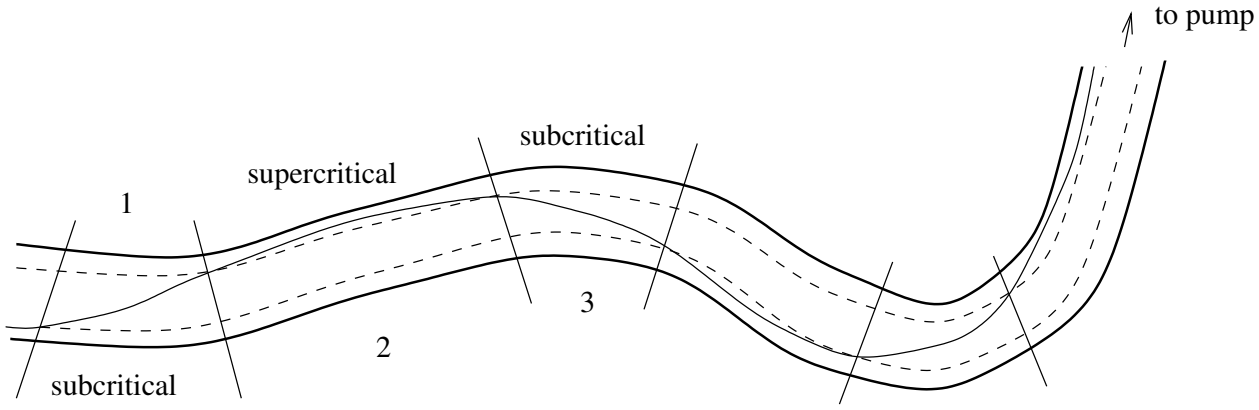

Figure 4.1: Sketch showing the position of the (straight-pipe) equilibrium hold-up as the pipe inclination slowly varies. The dotted lines indicate the zeros of $L(A)$. Note that as discussed this is not a possible steady state of the problem, and that the vertical scale is exaggerated.

showed that this proved not to be the case, and the point at which the stratified flow becomes linearly unstable does not vary significantly with the proportion of water cut. As the fraction of water varies from 0.35 to 0.55 the angle of inclination at which the flow becomes linearly unstable varies by 0.0002 radians or 0.0117°. Thus for a pipe where the inclination is varying by 1° per 100m this corresponds to the point at which instability occurs varying by at most 1.1m, which is negligible over the large length scale of the undulations in the well.

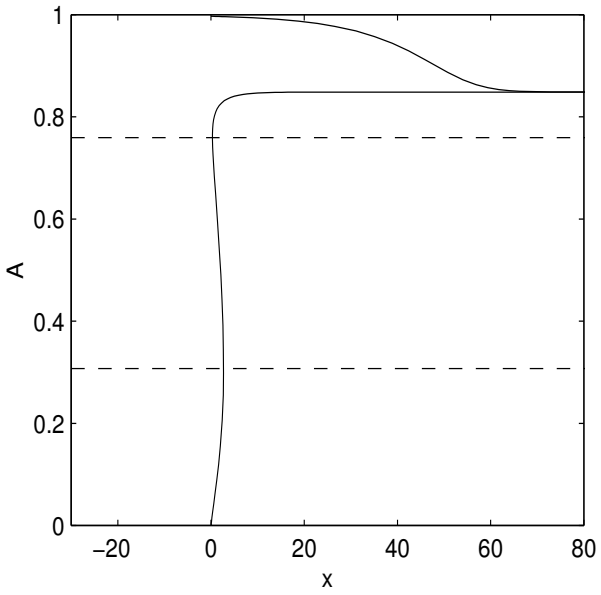

(a) 2° upflow

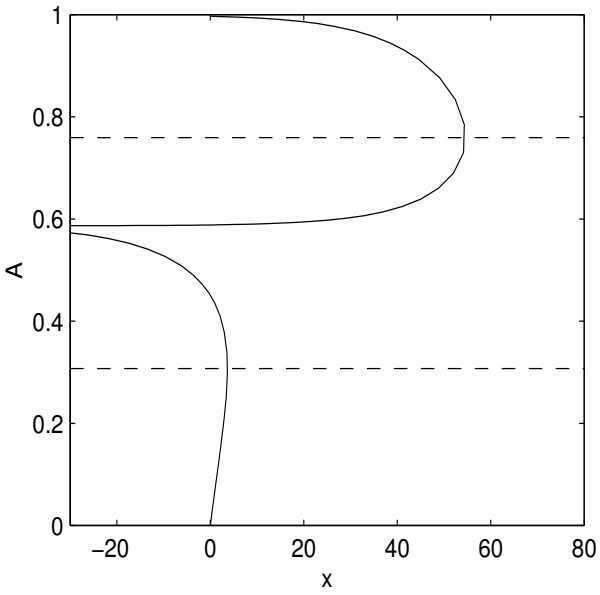

(b) horizontal flow

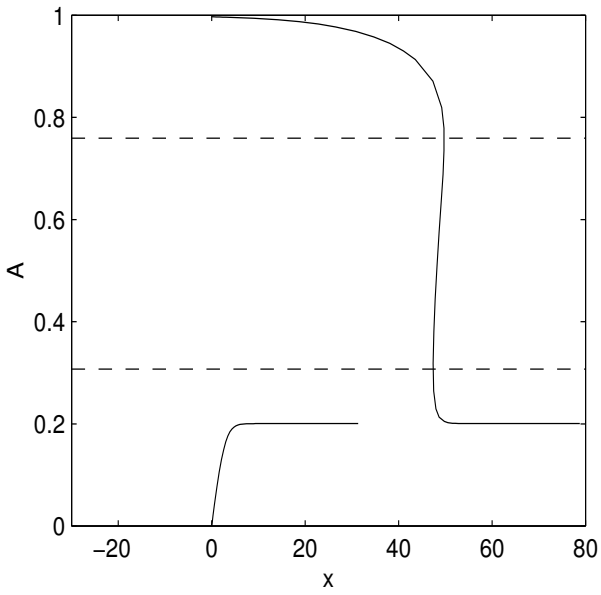

(c) 2° downflow

Figure 4.2: Profiles of steady state solutions (in a straight pipe) when $L(A)$ has a pair of zeros (dotted). These solutions are for $\beta = 40$, which corresponds to a total flow rate of 1500 bpd.

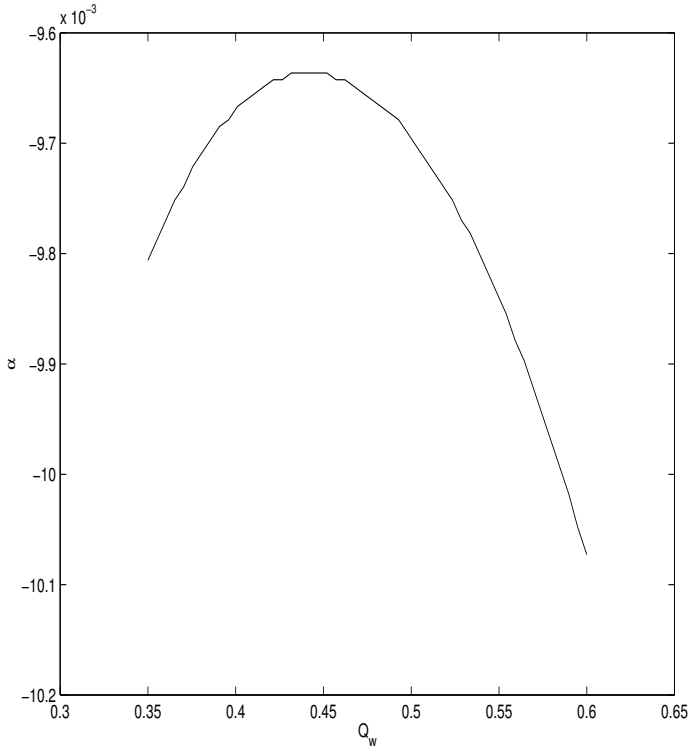

Figure 4.3: Plot of the value of α (in radians) at which the solution becomes linearly unstable for an upwards flow, against Q_w.

Chapter 5

Conclusions

In this chapter we briefly summarise the thesis, and outline areas in which further study may be fruitful.

5.1 Summary of work

In chapter one we have summarised the problem, and given an account of the experimental work which has been conducted into oil-water flows.

In chapter two we have formulated a one-dimensional model for oil-water two-phase flow, which accommodates source terms to model the influx of substances through perforations. We studied the equations governing steady states of the problem, and examined the linear stability of these steady states.

In chapter three we considered the possibility of roll waves forming as a result of this linear instability. Such roll waves were seen to be possible when the uniform flow was linearly unstable.

In chapter four we have given a brief outline of a possible solution of the problem. We have seen that the initially conjectured cause of the terrain slugging occurs at much lower total flow rates than in the case of the Wytch farms oil-well. We attempted to produce a mechanism for the terrain slugging, but this did not give a positive result.

5.2 Future work

Although the model gives solutions for uniform steady states which qualitatively agree with the initial data, the model predicts that such steady states are unstable when in practice they prove not to be. This is probably a result of the use of constant friction factors, as these terms both determine the hold-up of the steady state and influence

its stability. Comparing the results of this stability analysis (with suitably modified friction factors) with experimental data would be a profitable extension to the work.

Another area in which work could be conducted is in the boundary conditions on the well. It looks be possible to produce a condition relating the pressure in the well to the rate of influx through the perforations by considering a sink flow in the rock near the well. We also require suitable boundary conditions at the outlet of the pipe, which requires knowledge of the behaviour of the pump.

Through studying the possibility of roll waves being produced in an oil-water flow I have found that previous attempts to model a hydraulic jump in a liquid-liquid system are not conclusive. If such jumps are possible in an oil-water system then this appears to be an open problem.

We did consider a simple model for the large terrain slugging, but this did not prove to be successful. This may be a result of the linear instability analysis being inaccurate. In order to explain the large terrain slugging by means of such a density wave instability would require suitable boundary conditions at either end of the well (or at the perforations). We would also require some idea as to the nature of the flow in the regions for which the stratified flow is unstable, as we need a model for the flow in these regions as well. In particular we require an expression for the pressure drop for such a flow.

The problem of the non-existence of steady solutions at low flow rates is unsolved, and would probably have to be tackled by a numerical technique (possibly with a two or three dimensional model). This problem is unlikely to be the cause of the terrain slugging in the case of the Wytch Farms wells however.

5.3 Relationship to the thesis of Adam Dawlatly

The system of equations used by Adam Dawlatley in his thesis [15] is slightly different to those considered here due to the much smaller difference in density between the phases. It may be possible to form a model for discrete slugs of oil in a similar manner, but these have not been observed in any of the flow loop studies. If such a slug does resemble those in air-water flow then the jump conditions at the front of the slug are unclear. It seems more plausible that, if such slugs occur, they consist of a bubbly flow with varying water hold-up.

5.4 Final comments

In this thesis we have formulated a simple model for stratified two-phase flow, and identified a number of deficiencies and possible improvements. We have also found that the problem of terrain slugging is likely to require a model for the whole well, and not simply considering a problem restricted to a small section of the well.

Bibliography

[1] R. Aknoukh. Keeping producing wells healthy. *Oilfield Review*, pages 30–47, Spring 1999.

[2] P. Angeli and G.F. Hewitt. Flow structure in horizontal oil-water flow. *Int. J. Multiphase Flow*, **26**:1117–1140, 2000.

[3] L. Armi. The hydraulics of two flowing layers with different densities. *J. Fluid Mech.*, **163**:27–58, 1986.

[4] O. Baker. Simultaneous flow of oil and gas. *Oil Gas J.*, **53**:185, 1954.

[5] S. Bamforth. Revitalising production logging. *Oilfield Review*, pages 44–60, Winter 1996.

[6] D. Barnea and Y. Taitel. Structural and interfacial stability of multiple solutions for stratified flow. *Int. J. Multiphase Flow*, **18**(6):821–830, NOV 1992.

[7] D. Barnea and Y. Taitel. Interfacial and structural stability of separated flow. *Int. J. Multiph. Flow*, **20**:387–414, 1994.

[8] N Barret and D King. Oil/water slugging of horizontal wells - symptom, cause and design. *SPE 49160*, 1998.

[9] G.S. Benton. The occurence of critical flow and hydraulic jump in a multi-layered fluid system. *J. Meteror.*, **11**:139–150, 1954.

[10] A. Boudlal and A. Dyment. Weakly nonlinear interfacial waves in a duct of arbitary cross section. *Euro J. Mech B/Fluids*, **15**(3):331–366, 1996.

[11] N Brauner and D. Moalem Maron. Two phase liquid-liquid stratified flow. *Physicochemical Hydrodynamics*, **11**(4):487–506, 1989.

[12] G. Catala, B. Théron, G. Conort, and J. Ferguson. Fluid flow fundamentals. *Oilfield Review*, 1996.

[13] M.E. Charles, G.W. Govier, and G.W. Hodgeson. The horizontal pipeline flow of equal density oil-water mixtures. *Canadian Journal of Chemical Engineering*, **39**:27–36, Feb 1961.

[14] C.J. Crowley, G.B. Wallis, and J.J. Barry. Validation of a one-dimensional wave model for the stratified-to-slug flow regime transition, with consequences for wave growth and slug frequency. *Int. J. Multiphase Flow*, **18**(2):249–271, 1992.

[15] A.H. Dawlatly. *Gas-liquid flow in a near horizontal oilwell.* Master's thesis, University of Oxford, 1999.

[16] V. De Henau and G.D. Raithby. A study of terrain-induced slugging in two-phase flow pipelines. *Int. J. Multiphase Flow*, **21**(3):365–379, 1995.

[17] P.G. Drazin and W.H. Reid. *Hydrodynamic Stability.* Cambridge University Press, 1981.

[18] R.F. Dressler. Mathematical solution of the problem of roll-waves in inclined open channels. *Communications on Pure and Applied Mathematics*, **2**:149–194, 1949.

[19] Donald A. Drew and Stephen L. Passman. *Theory of multicomponent fluids.* Springer-Verlag, New York, 1999.

[20] Y.V. Fairusov, P. Adrenas-Medina, J. Verdejo-Fierro, and R. Gonzalez-Islas. Flow pattern transitions in horizontal pipelines carrying oil-water mixtures: Full scale experiments. *Journal of Energy Resources Tecvhnology - ASME*, **122**:169, 2000.

[21] A. C. Fowler. *Mathematical models in the applied sciences.* Cambridge University Press, Cambridge, 1997.

[22] A.C. Fowler. Linear and non-linear stability of heat exchangers. *J. Inst. Maths Applics*, **22**:361–382, 1978.

[23] D. Hasson, U. Mann, and A. Nir. Annular flow of two immiscible liquids. *Canadian Journal of Chemical Engineering*, **48**:514–520, October 1970.

[24] Q. Jiang and R.B. Smith. Ideal shocks in 2-layer flow. *Tellus*, **53A**(2):129–145, 2001.

[25] J.B. Klemp, R. Rotunno, and W.C. Skamarock. On the propagation of internal bores. *J. Fluid Mech.*, **331**:81–106, 1997.

[26] A.P.A. Kurban, P.A. Angeli, M.A. Mendes-Tatsis, and G.F. Hewitt. Stratified and dispersed oil-water flows in horizontal pipes. In *Proceedings of the 7th International Conference on Multiphase production*, pages 277–291. Mech. Eng. Publications, London, 1995.

[27] V.Yu. Lyapidevskii. The structure of roll waves in two-layer flows. *J. Appl. Maths Mechs.*, **64**(6):937–943, 2000.

[28] B.S. Massey. *Mechanics of Fluids*. Van Nostrand Reinhold, 1989.

[29] S.C. Mehrotra. Limitations on the existence of shock solutions in a two-fluid system. *Tellus*, **25**(2):169–173, 1973.

[30] S.C. Mehrotra and R.E. Kelly. On the question of non-uniqueness of internal hydraulic jumps and drops in a two-fluid system. *Tellus*, **25**(6):560–567, 1973.

[31] J.H Merkin and D.J. Needham. An infinite period bifurcation arising in roll waves down an open channel. *Proc. R. Soc. Lond. A*, **405**:103–116, 1986.

[32] Brauner N. and D. Moalem Marron. Stability analysis of stratified liquid-liquid flow. *Int. J. Multiphase Flow*, 1992.

[33] M Nadler and D. Mewes. Flow induced emulsification in the flow of two immiscible liquids in horizontal pipes. *Int. J. Multiphase Flow*, **23**(1):55–68, 1997.

[34] D.J. Needham and J.H. Merkin. On roll waves down an open inclined channel. *Proc. R. Soc. Lond. A*, **394**:259–278, 1984.

[35] T.S. Ng, C.J. Lawrence, and G.F. Hewitt. Interface shapes for two-phase laminar stratified flow in a circular pipe. *Int. J. Multiphase Flow*, **27**:1301–1311, 2001.

[36] T.W.F. Russell, G.W. Hodgeson, and G.W. Govier. Horizontal pipeline flow of mixtures of oil and water. *Canadian Journal of Chemical Engineering*, **37**:9–17, Feb 1959.

[37] Z. Schmidt, J.P. Brill, and H. D. Beggs. Experimental study of severe slugging in a two phase pipeline-riser pipe system. *SPE*, 1971.

[38] D.S. Scott. Properties of co-current gas-liquid flow. *Advances in Chemical Engineering*, **4**:199–277, 1963.

[39] P.L. Spedding and D.R. Spence. Flow regimes in 2-phase gas-liquid flow. *Int. J. Multiphase flow*, 1993.

[40] M. M. Stanišić. *The mathematical theory of turbulence*. Springer-Verlag, New York, second edition, 1988.

[41] J.J. Stoker. *Water waves*. Interscience, 1957.

[42] Y. Taitel. Stability of severe slugging. *Int. J. multiphase flow*, 1986.

[43] Y. Taitel and A.E. Dukler. A model for perdicting flow regime transitions in horizontal and near horizontal gas-liquid flow. *AIChE Journal*, **22**(1):47–55, 1976.

[44] B.E. Théron and T. Unwin. Stratified flow model and interpretation in horizontal wells. *SPE*, (36560), 1996.

[45] J.L. Trallero. *Oil-Water Flow Patterns in Horizontal Pipes*. PhD thesis, The university of Tulsa, 1995.

[46] J.L. Trallero, C. Sarica, and J. P. Brill. A studfy of oil-water flow patterns in horizontal pipes. *SPE*, (36609), 1996.

[47] G.B. Wallis. *One-Dimensional Two-Phase Flow*. McGraw-Hill, 1969.

[48] M Watson. Wavy stratified flow and the transition to slug flo. In *4th International Conference on Multi-phase flow*, number Paper G3, Nice, France, 1989.

[49] P.B. Whalley. *Two-Phase Flow and Heat Transfer*. Oxford Chemistry Primers. OUP, 1996.

[50] G.B. Whitham. *Linear and nonlinear waves*. Wiley-interscience, 1974.

[51] D.L. Wilkinson and I.R. Wood. A rapidly varied flow phenomenon in a two-layer flow. *J. Fluid Mech*, **47**(2):241–256, 1971.

[52] B. D. Woods, E. T. Hurlburt, and T. J. Hanratty. Mechanism of slug formation in downwardly inclined pipes. *Int. J. Multiph. Flow*, **26**:977–998, 2000.

[53] C.S. Yih and C.R. Guha. Hydraulic jump in a fluid system of two layers. *Tellus*, **7**(3):358–366, 1955.